A LINEAR ACCELERATOR EMPLOYING AN ELECTRODYNAMIC SPACE CHARGE EFFECT

Norbert Richard Heese

A THESIS

in

The Department

of

Physics

Presented in Partial Fulfillment of the Requirements for
the Degree of Doctor of Philosophy at
Sir George Williams University
Montreal, Canada

July, 1972

A LINEAR ACCELERATOR EMPLOYING AN ELECTRODYNAMICAL SPACE CHARGE EFFECT

ABSTRACT

A simple linear accelerator for electrons was built and is now in operation. The acceleration is accomplished by an electrodynamical space-charge effect in a cylindrical electron beam, by virtue of which the energy of the beam is transferred to the front electrons. The 7 ft.-long instrument, operated with a 20 keV, 350 mA beam, produces electrons of energies up to 14 MeV. Design and operational characteristics are presented along with the results of performance tests.

ACKNOWLEDGEMENTS

The author would like to thank Professor W.R. Raudorf for suggesting the project and for his continued aid, encouragement and advice throughout the course of research. Thanks are due to Mr. A. Coutu for his help in the early stages of this project.

The author is very much indebted to Messrs. J. Blaison, J. Loustau and A. Christodoulopoulos for their invaluable skill and help with the constructional phase of this work.

TABLE OF CONTENTS

STATEMENT OF ORIGINALITY

To the best knowledge of the author this is the first time that a linear accelerator utilizing a collective space-charge effect has been designed, constructed, and put into operation, which accelerates electrons to energies in the MeV range. Both design and construction of the device can therefore be considered to be original.

LIST OF FIGURES

Page

1. INTRODUCTION

In 1951[1] a novel method for accelerating electrons was proposed and discussed. According to this method the energy which is associated with an advancing cylindrical beam of electrons is transferred to the electrons at the front of the beam by virtue of a collective electrodynamical space-charge effect, hereafter referred to as Ram Effect (RE). The apparatus based upon this effect appears to be the electrical analogue of the hydraulic ram and was therefore called Electronic Ram (ER). Subsequently various models of an accelerator of the above type were built and operated to investigate systematically the principle underlying the proposed acceleration method.[2-4] The results of the experimentation with these models verified the occurrence of the RE and confirmed the physical picture of the acceleration process as described in the first paper on the subject. In view of these encouraging results it was decided to develop an ER which was capable of accelerating electrons to energies up to 10 MeV in contrast to the models which produced electrons of energies up to 20 keV only. Such an accelerator would combine small size with low cost, would be easy to operate and maintain, and soon become a unique instrument with a wide variety of applications.

The purpose of this work is to present and discuss:

(a) Design and construction of an ER of practical significance.

(b) Operational characteristics.

(c) The results of energy measurements.

1-2. Basic Structure of the ER.

A schematic view of the instrument is shown in Fig. 1. It consists essentially of the following components. An electron gun of cylindrical symmetry at one end of an evacuated tube (drift tube) which is very long relative to its diameter, and a coaxial tubular electrode (decelerator) on the other end, its length being several times larger than its diameter which is the same as that of the drift tube. The decelerator is electrically insulated against its cylindrical envelope, whose diameter is several times that of the drift tube. The metal drift tube and the housing of both cathode and decelerator are grounded during operation. All components are of cylindrical symmetry, and are made of non-magnetic material. The electron gun serves to project a coaxial cylindrical stream of electrons of predetermined velocity into and through the drift tube. The dominant feature of the design is the employment of a static axially symmetric magnetic field. This field, generated by means of suitable solenoids around the electron gun, drift tube and decelerator, is uniform in the drift tube, vanishes in the region of the cathode of the electron gun, rises rapidly to its greatest value in the region of the decelerator and falls off to zero towards the aluminum disk (exit window) which terminates the ER.

1-3. Principle of Operation.

The operation of the ER may be summed up as follows.

Figure 1

Schematic of the ER, not to scale.

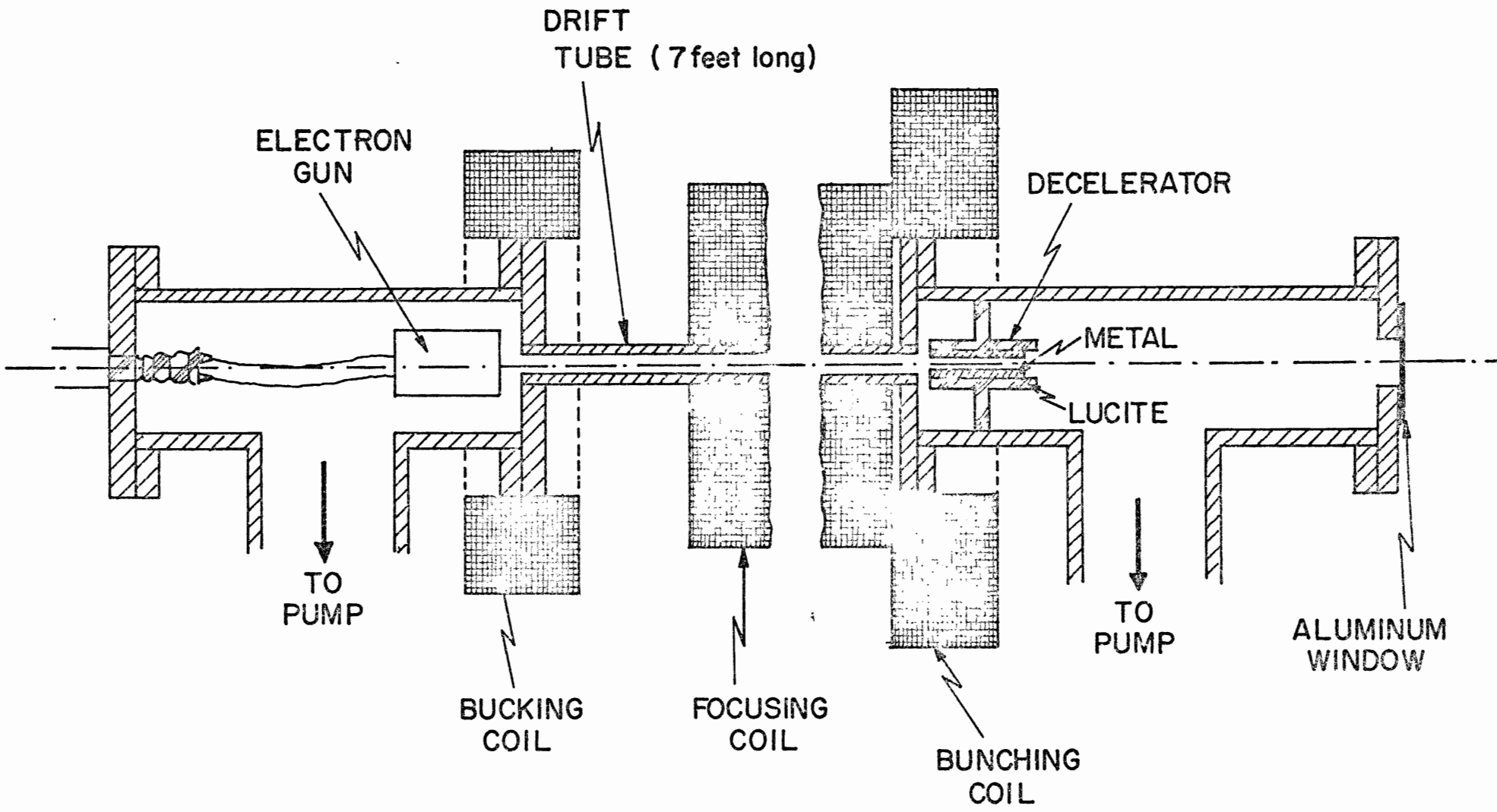
DRIFT
TUBE (7 feet long)
ELECTRON
GUN
DECELERATOR
METAL
LUCITE
TO
PUMP
TO
PUMP
ALUMINUM
WINDOW
BUCKING
COIL
FOCUSING
COIL
BUNCHING
COIL

Under the influence of the steady magnetic field, the electrons projected by the electron gun form as they enter the drift tube a cylindrical beam of uniform charge density. All the electrons in the beam rotate about the axis with the same angular velocity and approach the decelerator with the same axial velocity. In other words they form a steady cylindrical beam which rotates about its axis as a unit and advances in the same manner as a screw, the pitch being determined by the flux density of the focusing magnetic field within the drift tube.[5]

Arriving at the decelerator (its role being explained below) where the flux density increases rapidly in the direction of the stream, the strong radial component of the magnetic field brings about a complete conversion of axial to angular velocity of the electrons constituting the front portion of the beam. The focusing longitudinal component of the field on the other hand causes, due to the Lorentz force, a compression of that portion of the beam which revolves without advancing, and thereby an increase of the space-charge density. A potential barrier develops which blocks the passage into the decelerator, and against which the succeeding electrons ram. Both space-charge density and potential barrier continue to grow rapidly. Finally a space-charge limited cathode is formed, the potential of which is far below that of the decelerator. The electric field beyond the virtual cathode generated at the expense of the energy associated with the entire beam, draws electrons from the virtual cathode and accelerates them through

the decelerator. As they travel towards the aluminum window they encounter magnetic field conditions which are antisymmetric to those at the cathode. The radial component of the decreasing magnetic field there changes the angular velocity of the electrons back to axial velocity. Electrons of sufficiently high energy pass through the aluminum window and continue to travel outside the ER. A detailed discussion of the mechanism of the acceleration process and the underlying theoretical considerations are found in the original paper (Raudorf 1951). During the discharge the virtual cathode disintegrates, the decelerated beam disperses under the influence of the radial interelectronic forces, another beam is formed and the whole process is repeated. In the course of operation stray electrons charge up the decelerator negatively with respect to ground. The retarding electric field produced in this way and the larger diameter of the envelope assist in setting up the virtual cathode in front of the decelerator.[4]

2. DESIGN OF THE ELECTRONIC RAM

2-1. General Description.

Guided by the experience gained from the experimentation with ER models, it was decided to allow great variability to the flux densities of the applied magnetic fields, the injection energies of the electrons, and the emission of the cathode. Also the device should be constructed so that important components are readily accessible for readjustment and repair. The apparatus is therefore composed of three sections, (i) the electron gun, (ii) the drift tube, (iii) the decelerator. Part of the research program was to check the dependence of the maximum energy of the output electrons on the length of the beam. For this reason the drift tube is composed of two sections of equal length (not shown in Fig. 1) to permit operation with half the beam length after removal of one of the two sections. Standard Varian flanges and copper O-ring seals were used to join the various parts vacuum tightly together. Any readjustment to the cathode necessitates the removal of the gun and its exposure to air. Oxide coated cathodes are susceptible to poisoning and are easily damaged by ion bombardment, hence a directly heated pure tungsten filament was chosen as cathode. Projection of a cylindrical beam on the other hand requires a plane circular emissive surface, coaxial with the beam. This surface should be an equipotential surface, free from the magnetic field generated by the filament current. The electron optics of the electron gun should accomplish the

formation of a cylindrical beam of less than $\frac{1}{2}$ in. in diameter. Under certain operating conditions, however, magnetic concentration of the beam in addition to the electrostatic focusing may be necessary. A short solenoid (Bucking Coil) around the housing of the electron gun provides the possibility for additional beam collimation. For reasons given later, the field produced by the bucking coil must be negligibly small in comparison to that within the drift tube. The solenoids around the drift tube are designed so that longitudinal flux densities of up to 2000 G can be generated without overheating the coils. In front of the decelerator the flux density has to be raised above the "critical" or "limiting" value, that is the value at which the axial velocity of the arriving electrons is completely converted to angular velocity. For this purpose a suitably designed solenoid (Bunching Coil) is placed around the end portion of the system. The section containing the decelerator is terminated by a stainless steel flange with an aperture of $1\frac{1}{2}$ in. in diameter. This aperture is hermetically sealed with an aluminum window through which only electrons of energies above 524 keV can escape.

Independent power supply units are used to allow for the energizing of the various solenoids. During operation the drift tube as well as the metal envelope of the other sections are at ground potential. The decelerator, however, is well insulated against its housing, to enable it to charge up negatively during operation. Filament and filament supply must also be insulated,

since a voltage of at least 20 kV is applied to the filament during operation. A center-tapped transformer supplies the filament power which is controlled by a Variac on the primary side. High vacuum is imperative for a successful operation of the ER. Efficient pumps, fitted with a liquid nitrogen cooled baffle, are therefore employed.

2-2. Components and Constructional Details.

Electron Gun. Searching for a suitable electron gun, it turned out that the Veeco Electron Gun Model VeB-6 and its matching power supply met all the requirements called for reasonably well. It was therefore decided to equip the accelerator with this commercially available gun and power supply. As is obvious from the cross-section presented in Fig. 2, the gun is of a modified Pierce design, using a directly heated tungsten filament. The filament itself is wound in the shape of a bifilar spiral, to approximate an equipotential cathode, and to reduce the magnetic field due to the filament current to a minimum. The gun, as specified by Veeco, is capable of producing a beam of 300 mA at a voltage of -20 kV between filament and grounded anode, with the focusing electrode at the same potential as the filament. A slight modification was made for use in this apparatus in that the filament was moved closer to the anode by 2 mm. This did not noticeably affect the electron optics, but it made it possible to draw a current of about 650 mA at a voltage of -24 kV.

Referring to Fig. 2, the gun was set in a circular depression

Figure 2

Cross-section of the Electron Gun (Actual Size). Inset: Configuration of the Filament.

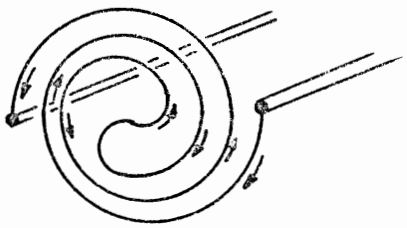

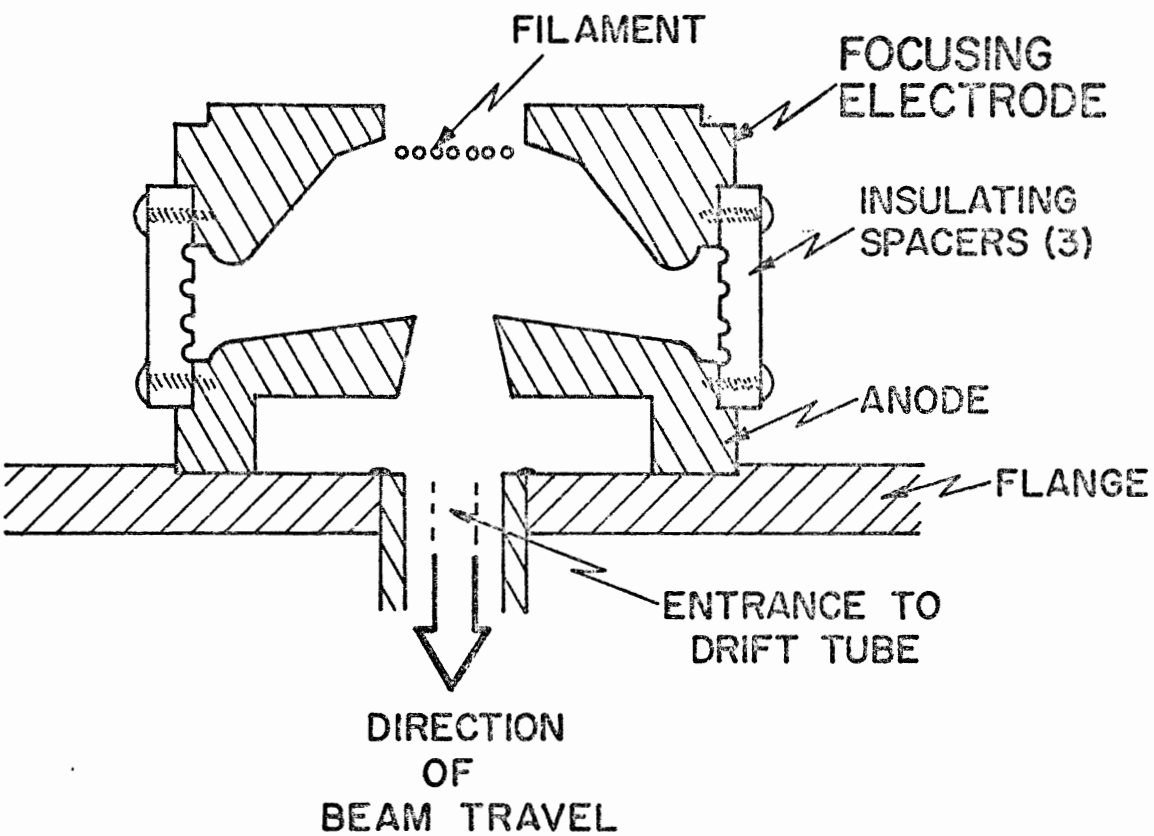
FILAMENT
FOCUSING ELECTRODE
INSULATING SPACERS (3)
ANODE
FLANGE
ENTRANCE TO DRIFT TUBE
DIRECTION OF BEAM TRAVEL

Figure 3

Block Diagram of the Electron Gun

Power Supplies.

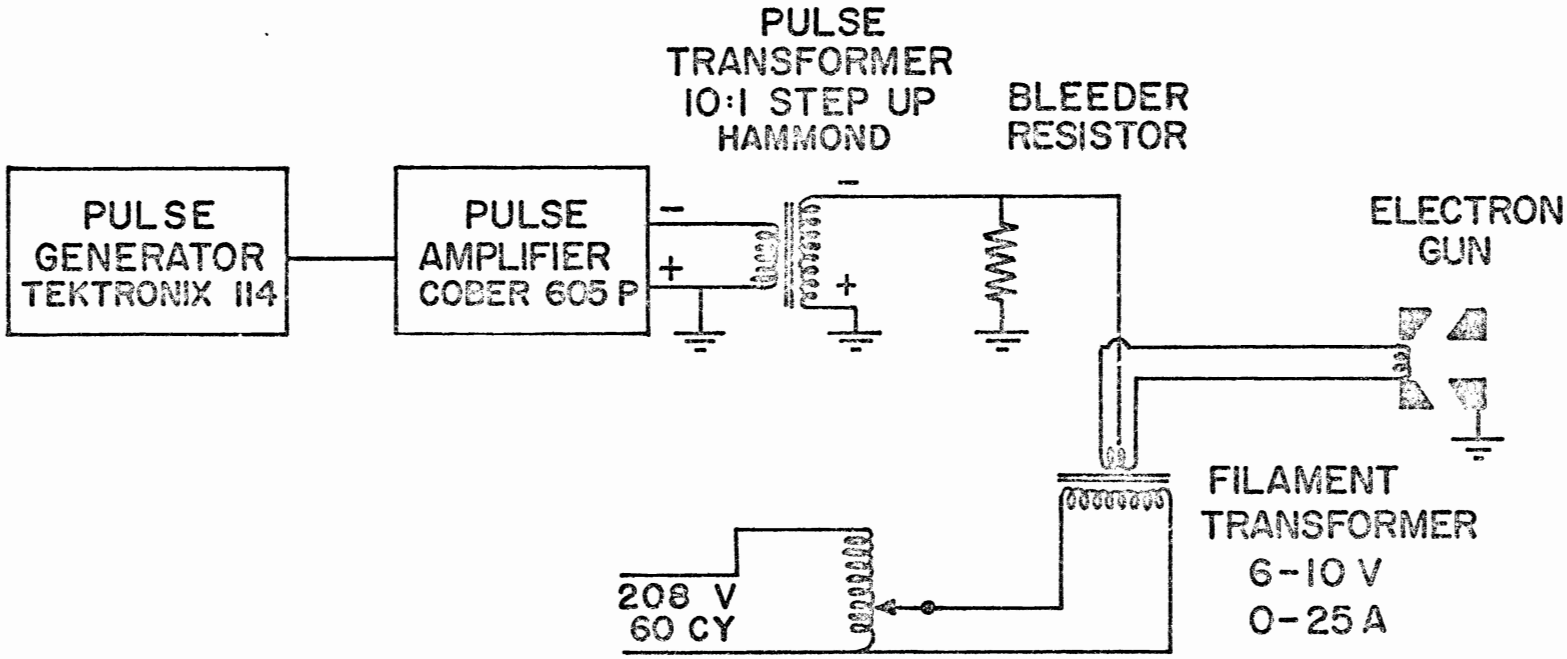
PULSE TRANSFORMER 10:1 STEP UP HAMMOND
BLEEDER RESISTOR
PULSE GENERATOR TEKTRONIX 114
PULSE AMPLIFIER CODER 605 P
ELECTRON GUN
FILAMENT TRANSFORMER 6-10 V 0-25 A
208 V 60 CY

on the inside face of the flange, and was firmly clamped into place, coaxially with respect to the drift tube. The components of the gun were made of highly polished stainless steel, whereas the three insulating spacers were of high density ceramic.

Pulsing System. The gun was operated in a pulsed mode only to overcome the problem of heat dissipation. As indicated in the block diagram of Fig. 3, the square pulses generated by a Tektronix Model 114 pulse generator are fed into a high power pulse amplifier (Cober Electronics Model 605 P). The amplified square pulses of more than 2000 V amplitude at 10 A pulse current are then stepped up to more than 20 kV at 1 A by a specially designed pulse transformer. The output voltage of the pulse transformer is then applied to a centertap on the secondary windings of the filament transformer, whose terminals are connected through a specially designed cable and vacuum feedthrough to the gun. The non-inductive bleeder resistor shown in Fig. 3 serves to match impedances and thus to improve the pulse shape.

The electron gun and feedthrough are housed in a Varian T - section of 4 in. outer diameter, Model 952-5042 as shown in the schematic in Fig. 1, and on the photograph (Fig. 4) of the gun section of the ER. The T - section is pumped through a 90° elbow (Varian Model 952-5040) which is connected through a stainless steel pipe of 4 in. outer diameter to the lower flange of the special vacuum manifold (Fig. 5).

Figure 4

View of the Electron Gun End of the ER. A Portion of the Beam Tube is visible between the first Aluminum Support and the Flange under the Bucking Coil.

Figure 5

Details of custom-built Vacuum Manifold

by Varian Corp.

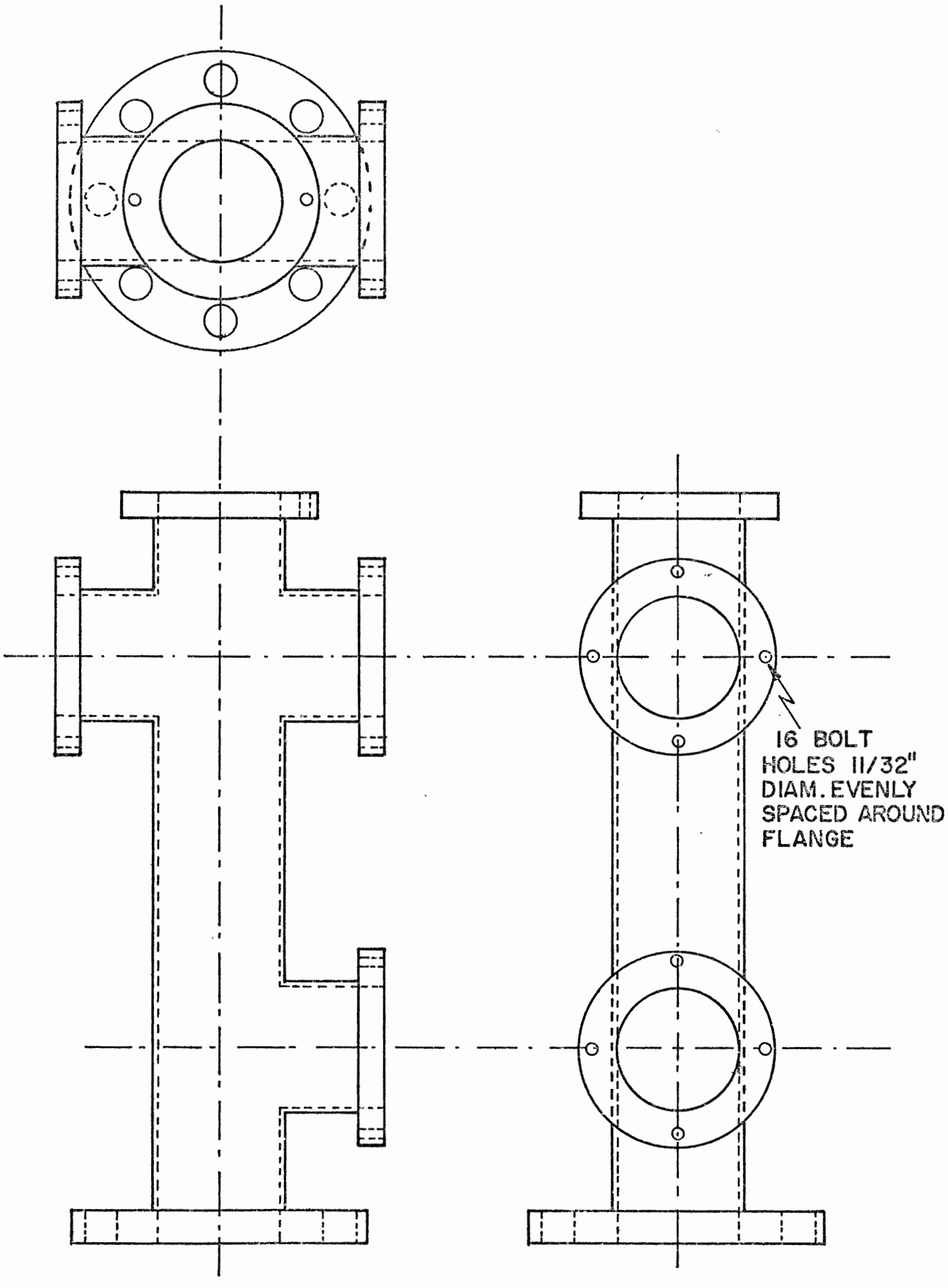
16 BOLT
HOLES 11/32"
DIAM. EVENLY
SPACED AROUND
FLANGE

Bucking Coil. In order to be able to control the magnetic field at the cathode, a special coil was built and fitted around the flange to which the electron gun is bolted. The coil consists of 1740 turns of 18 gauge wire, wound on a form 3 in. wide and of 6 in. inner diameter. For example, a field of 105 G appears at the cathode when the focusing coils are fully energized. The flux density can be reduced to zero by an opposing field produced by a current of 1 A through the bucking coil.

The Drift Tube. The drift tube consists of two sections. Each section is made of a 44 in. long stainless steel tube of 3/4 in. outer diameter, and a wall thickness of 1/8 in. The length of the focusing coil surrounding each section is 40 in. Five brass flanges of 3 3/4 in. outer diameter (Fig. 6) are welded along the length of each drift tube section. Over these a brass tube of 4 in. outer diameter is slid with corresponding flanges of 7 7/8 in. diameter on its outside. The outside flanges are held by heavy aluminum supports which are bolted to a 3/4 in.-thick aluminum plate serving as a rigid table for the entire assembly (Figures 4 and 7). In this fashion the rigidity and straightness of the drift tube are assured. When the construction of the ER was completed, the linearity of the assembly was checked with a transit and was found to deviate from perfect alignment at the most by $\pm$ 0.005 in.

The four spaces between the inside flanges accommodate the inner coils, each of which is evenly wound with 12 gauge insulated magnet wire. All four coils are connected in series and thus

Figure 6

Drift Tube and Focusing Coil Assembly

(Actual Size).

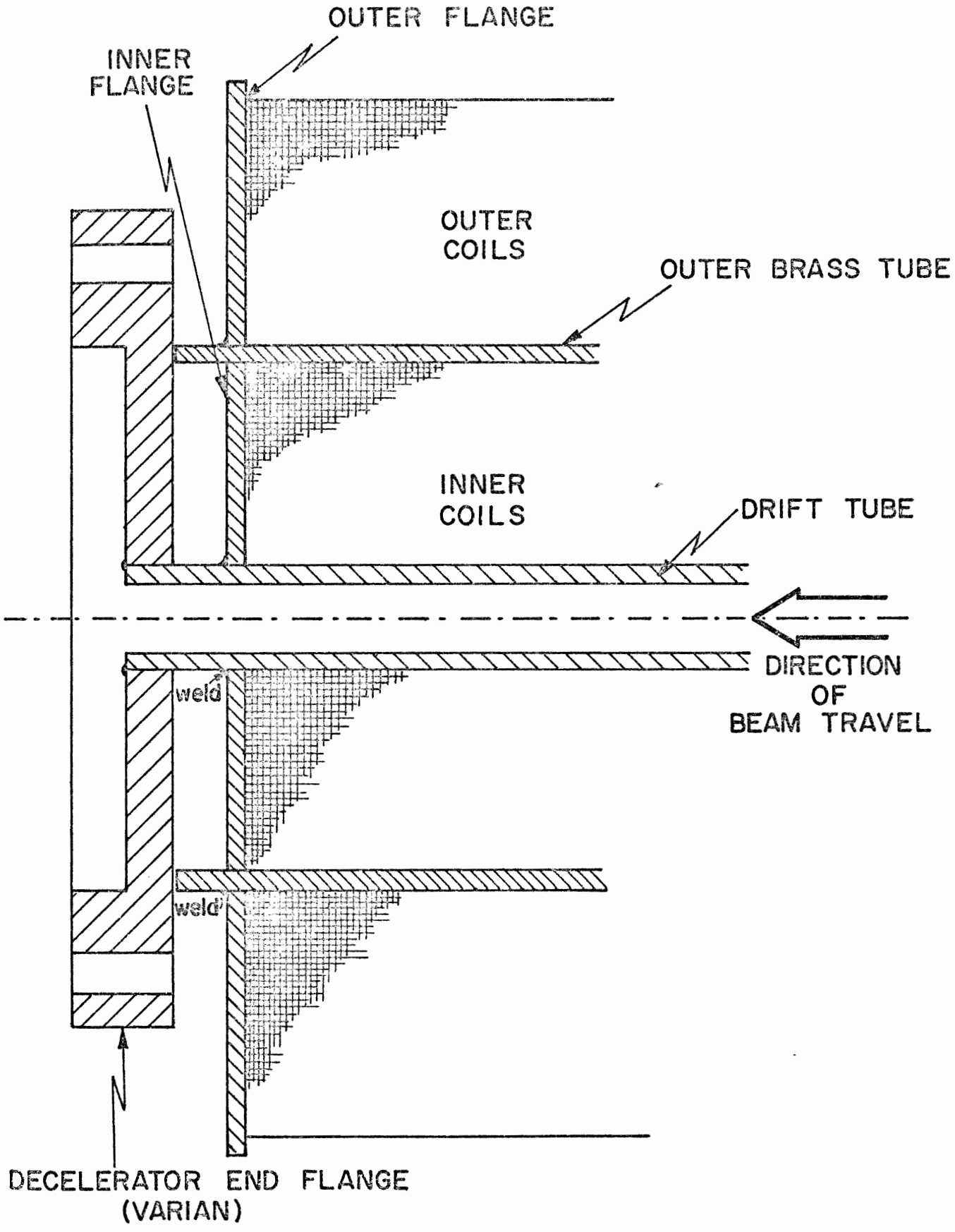
OUTER FLANGE
INNER FLANGE
OUTER COILS
OUTER BRASS TUBE
INNER COILS
DRIFT TUBE
DIRECTION OF BEAM TRAVEL
weld
weld
DECELERATOR END FLANGE (VARIAN)

constitute a solenoid of 1 m length with 17 layers of 460 turns each. With an energizing current of 10 A, this solenoid alone produces an axial magnetic field of 975 G.

Similarly the outer solenoid consists also of four coils. Each of them has 21 layers, and each layer 115 turns; these coils are connected in parallel, and, when energized with a current of 10 A per coil, generate an axial field of 1025 G. Hence both solenoids together produce, if operated as above, a flux density of 2000 G within the drift tube.

The outer coils were driven by a Hewlett-Packard Model 6459 A, 0-64 V, 0-50 A powersupply, while the inner solenoid was energized by a shop-built 0-100 V, 0-10 A powersupply.

As previously mentioned, the drift tube consists of two fully equivalent sections joined together with the aid of flanges and O-ring seals. To assure a uniform magnetic field, a small auxiliary coil was fitted into the gap between the solenoids of the two sections (Fig. 7). The solenoids of each section are driven by equivalent powersupplies.

The Decelerator. Referring to Figure 8, the decelerator consists of a piece of stainless steel tubing of the same diameter and wall thickness as the drift tube, $2\frac{1}{2}$ in. in length. It is fitted firmly into a tubing of lucite, and the entire assembly is supported rigidly and coaxially with respect to the drift tube

Figure 7

Overall View of the ER.

The Exit Window is hidden behind the Deflecting Magnet.

by a three-legged "spider" of polystyrene. The spacing between the end of the drift tube and the decelerator is 3/16 in. Considerable care was taken to assure that the decelerator axis was precisely aligned with that of the drift tube. The interior wall of the decelerator was threaded to reduce secondary emission of electrons. In general, the secondary emission coefficient for a given material is highest at grazing incidence of the primary electrons, which can be avoided to a great extent by threading the inner surface of the tube.

The Bunching Coil. To produce a rapid increase of the magnetic flux density at the entrance to the decelerator, and to focus the accelerated electrons, a large solenoid was placed over the housing of the decelerator. The solenoid is 3 in. wide and of 6 in. inner diameter, and is wound with 3500 turns of 18 gauge wire. Fully energized it can raise the field intensity in the region between the end of the drift tube and the decelerator to 2500 G.

Exit Window and Lead Collimators. The high energy electrons traverse the decelerator and travel towards the exit window. This consists simply of a sheet of aluminum, 0.025 in. thick (173 mg/cm^2), covering a $1\frac{1}{2}$ in. diameter hole in the end flange. It is held in place by an aluminum ring, to which a support is attached at a distance of $2\frac{1}{4}$ in. This support serves to clamp collimating lead disks into position, as shown in Fig. 8. The first collimator has a hole $\frac{3}{4}$ in. in diameter, while the other two have holes of only $\frac{1}{4}$ in. in diameter; the thickness of each disk is $\frac{1}{4}$ in. The positions and spacing of

Figure 8

Cross-section through the Decelerator

End of the ER ($\frac{1}{2}$ Actual Size).

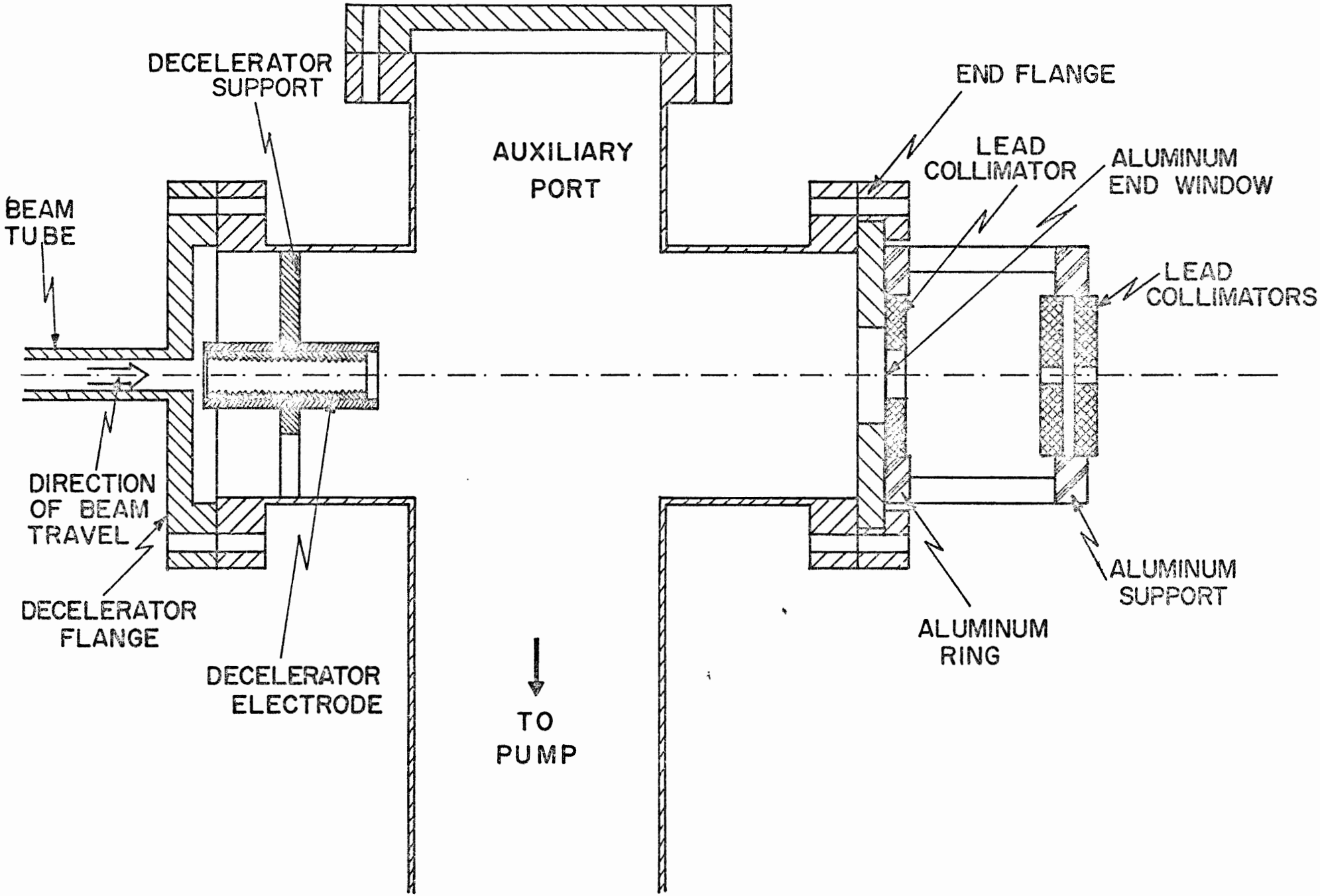
DECELERATOR SUPPORT
AUXILIARY PORT
END FLANGE
LEAD COLLIMATOR
ALUMINUM END WINDOW
BEAM TUBE
LEAD COLLIMATORS
DIRECTION OF BEAM TRAVEL
DECELERATOR FLANGE
DECELERATOR ELECTRODE
TO PUMP
ALUMINUM RING
ALUMINUM SUPPORT

the lead disks are evident in Fig. 8.

The Vacuum System.

(a) Manifold: The apparatus described in the previous section is housed in the upper part of the vacuum manifold, which is a special construction by Varian Associates. Its schematic is shown in Fig. 5, and also in the foreground of Fig. 7, with the deflecting magnet in position. Quite evident in this photograph is also the bunching coil around the decelerator housing. Just below the table, barely visible, is the lower connection to the vacuum manifold through which the electron gun chamber is pumped.

(b) Vacuum pump and monitoring system: Since the acceleration of electrons is based on the collective effect of negative space-charge, the efficiency of the acceleration process suffers seriously from the presence of positive ions. A high vacuum within the accelerator is therefore of the utmost importance.

The vacuum pump used in this work is the NRC self-fractionating oil diffusion pump Model NHS 4, backed by a Welch mechanical pump Model 1397. The diffusion pump is fitted with a liquid nitrogen cooled baffle (NRC Model 0315-1-4) and a 4 in. hand operated high vacuum slide valve (NRC Model 1293 S) for system

isolation. In addition, suitable roughing and foreline valves are employed.

The vacuum seals at all flanges are copper gaskets clamped between steel knife edges, with the exception of one neoprene O-ring at the exit window. After extensive degassing, the pumps are able to maintain a pressure of 0.2 μTorr during operation of the ram. The vacuum is monitored by an NRC Model 831 ionization gauge in conjunction with the NRC Model 563-SK ionization gauge tube. Appropriate thermocouple gauges for rough vacuum monitoring are used as well.

3. OPERATIONAL CHARACTERISTICS

3-1. Measurements Inside the ER.

It is known that a high density electron beam cannot be projected over large distances under the influence of an electric field alone without appreciable dispersion. The successful operation of the ER, however, requires a steady cylindrical beam of uniform space-charge density, in which the axial velocity of all electrons is the same, and in which the space-charge repulsive forces are balanced by magnetic focusing forces, so that the beam may be made as long as desirable without any appreciable change in its cross-section.

The dominant feature of the method of producing such a beam is the utilization of a steady axial magnetic field which has the following properties: It vanishes at the source of the electrons, is coaxial with respect to the electron stream and substantially longitudinal for an axial distance in the direction of the stream, the distance being very large relative to the diameter of the stream. Under these conditions the equations of motion of an electron are readily found which combined with the energy equation, determine the properties of the beam. (Appendix I.) It turns out that the electrons in the beam revolve around the beam axis with just the required angular velocity to balance the coulomb forces. The angular velocity is proportional to the flux density, and the space-charge density is proportional to the square of the flux

density. Therefore, if the beam is immersed in a uniform axial field, the angular velocity is the same for all electrons in the beam, and the space-charge density is uniform. The axial velocity is also the same for all electrons; it is the smaller, the greater the flux density of the applied magnetic field. As the flux density increases, the energy of the beam is more and more transformed into rotational energy. If the flux density equals or exceeds the critical value, the axial velocity of the beam is reduced to zero, and the beam cannot advance.

The measurement of the variation of the beam current with axial distance from the electron gun was accomplished with the sliding probe shown in Fig. 9 (a). A $\frac{1}{4}$ in. steel rod, 56 in. long, was polished to a shiny finish, and was attached to a short cylindrical brass cup of slightly smaller diameter than the inner diameter of the drift tube. A teflon spacer right behind the cup prevented contact of the probe with the wall. Two other similar spacers further back guarded against sagging of the steel rod. The seal consisted of two neoprene O-rings pressed around the rod by a bakelite sleeve through which the rod was passed. This seal allowed the probe to be moved backwards and forwards inside the drift tube while the system was evacuated. An ammeter between probe and ground measured the beam current as dependent on position by sliding the probe along the tube. A series of measurements with the probe at both ends of the drift tube and intermediate positions showed, as expected, no appreciable variation of the beam current

Figure 9

(a) Details of Sliding Probe for Beam Measurements inside the Drift Tube.

(b) Constructional Details of Exterior Collecting Cup.

Both $\frac{1}{2}$ Actual Size.

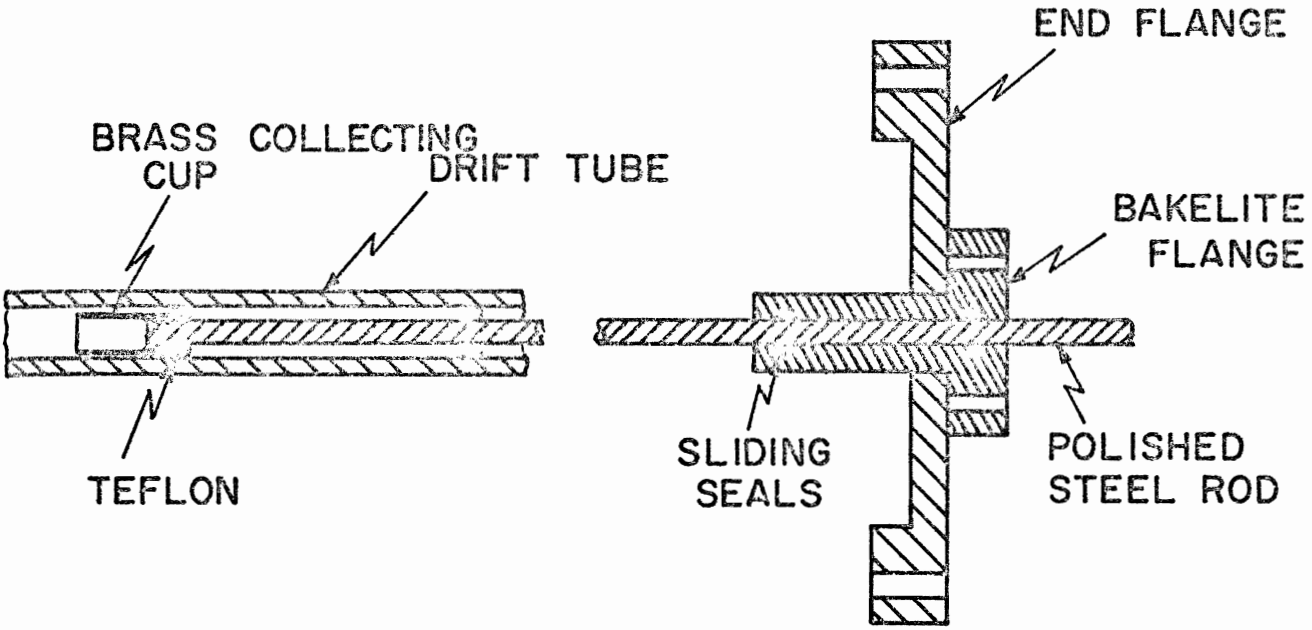
END FLANGE
BRASS COLLECTING CUP
DRIFT TUBE
BAKELITE FLANGE
TEFLON
SLIDING SEALS
POLISHED STEEL ROD

(a)

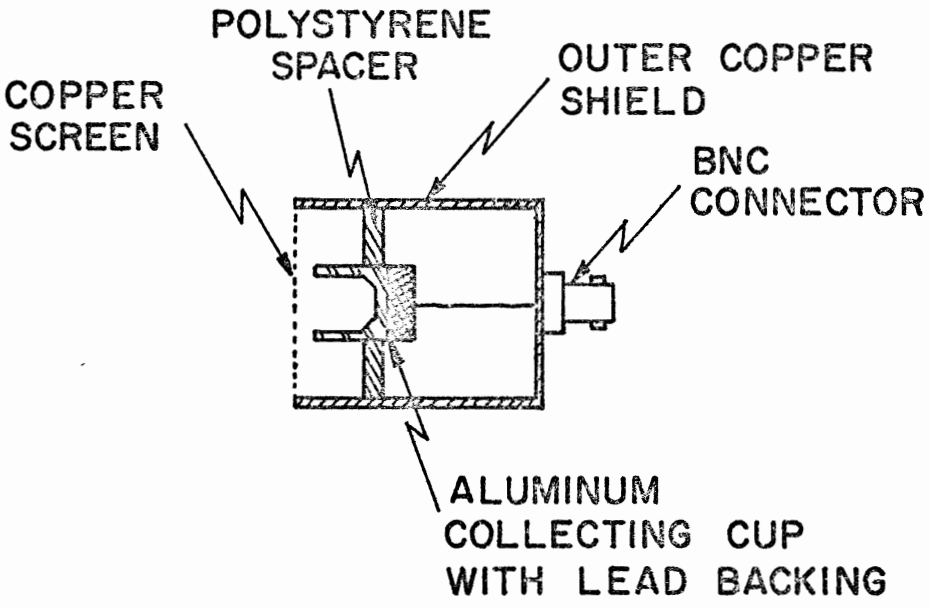
POLYSTYRENE SPACER
OUTER COPPER SHIELD
COPPER SCREEN
BNC CONNECTOR
ALUMINUM COLLECTING CUP WITH LEAD BACKING

(b)

Figure 10

Beam Current Pulse as detected with Sliding Probe. Voltage across 15 ohms.

Vertical Sensitivity: 5 V/cm

Horizontal Scale: 5 μsec/cm

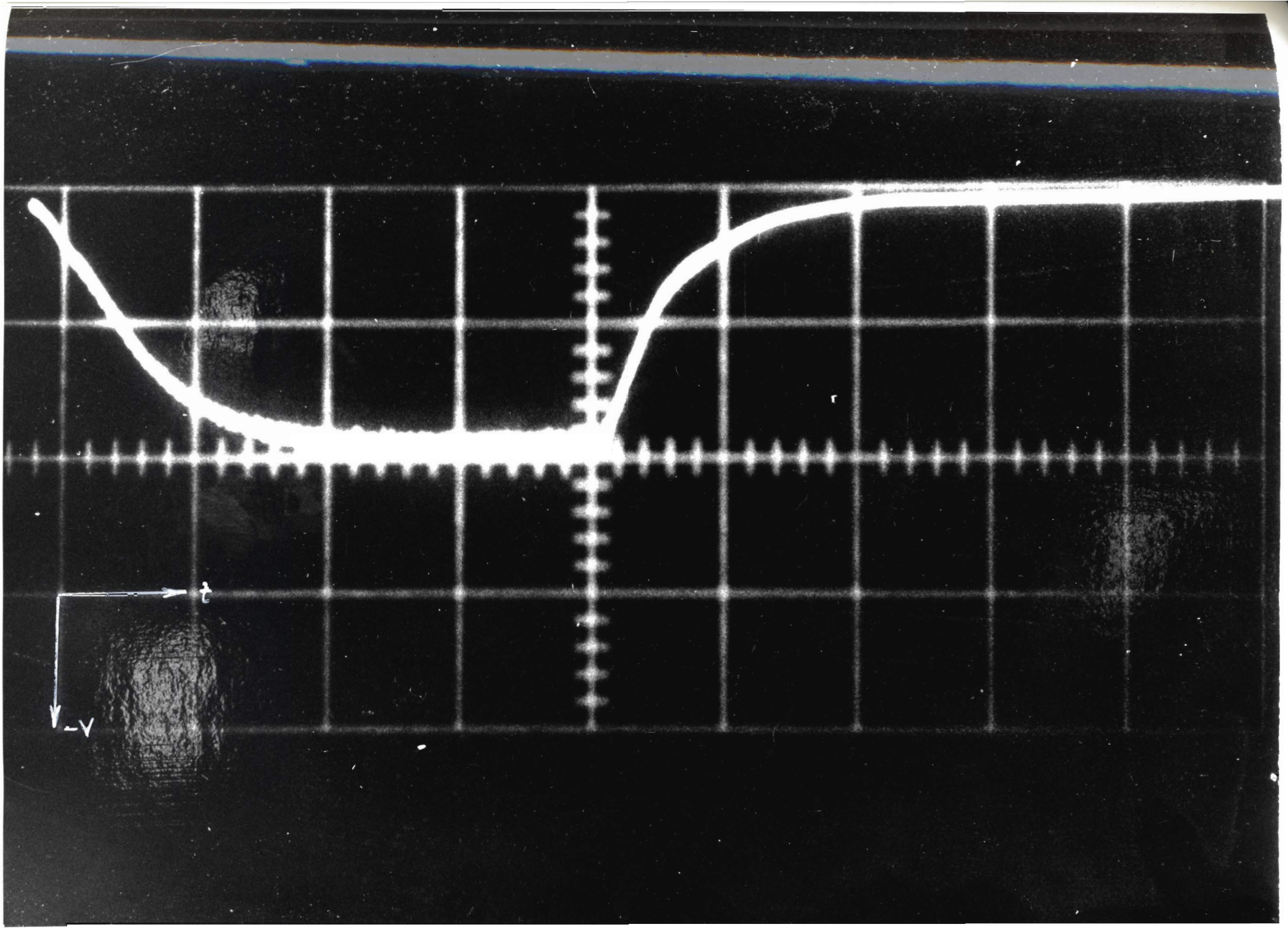
t
-V

along the drift tube, provided the flux density of the applied focusing magnetic field was properly chosen.

The oscillogram in Fig. 10 shows a typical voltage pulse across 15 ohms, obtained with the probe inside the drift tube. The output of the pulse generator consisted of square pulses of 30 usec duration and 26 kV-amplitude, the inevitable reactances, however, of the cable connecting the secondary of the filament transformer to the electron gun caused the obvious distortion of the original shape. The peak value of the beam current in this case was 680 mA. When the probe was at the entrance of the drift tube, the beam current dropped to 653 mA, as can be seen from the oscillogram. Measurements taken at the end as well as at the center of the drift tube did not reveal any significant deviation from this value. Axial focusing magnetic field during these measurements happened to be 2000 G within the drift tube, and 25 G at the cathode.

In order to check on the occurrence of the RE, a specifically designed hollow cylindrical collector was mounted coaxially with respect to the decelerator on the terminating flange of the ER (Fig. 11 (b). The collector was made from a single piece of brass, equipped with a cooling fin and mounted on a glass-to-metal seal. Its terminal was connected to the input of a Tektronix Oscilloscope, type 454 A, and to ground via a 15 ohm resistor. The bucking coil, focusing coils and bunching coil were optimally energized. The oscillograms in Fig. 12 (a) and (b), which were taken on different days show the output when the cathode was pulsed with a square wave

Figure 11

(a) Configuration of Tungsten Anode.

(b) Details of interior Collecting Cup.

Both ½ Actual Size.

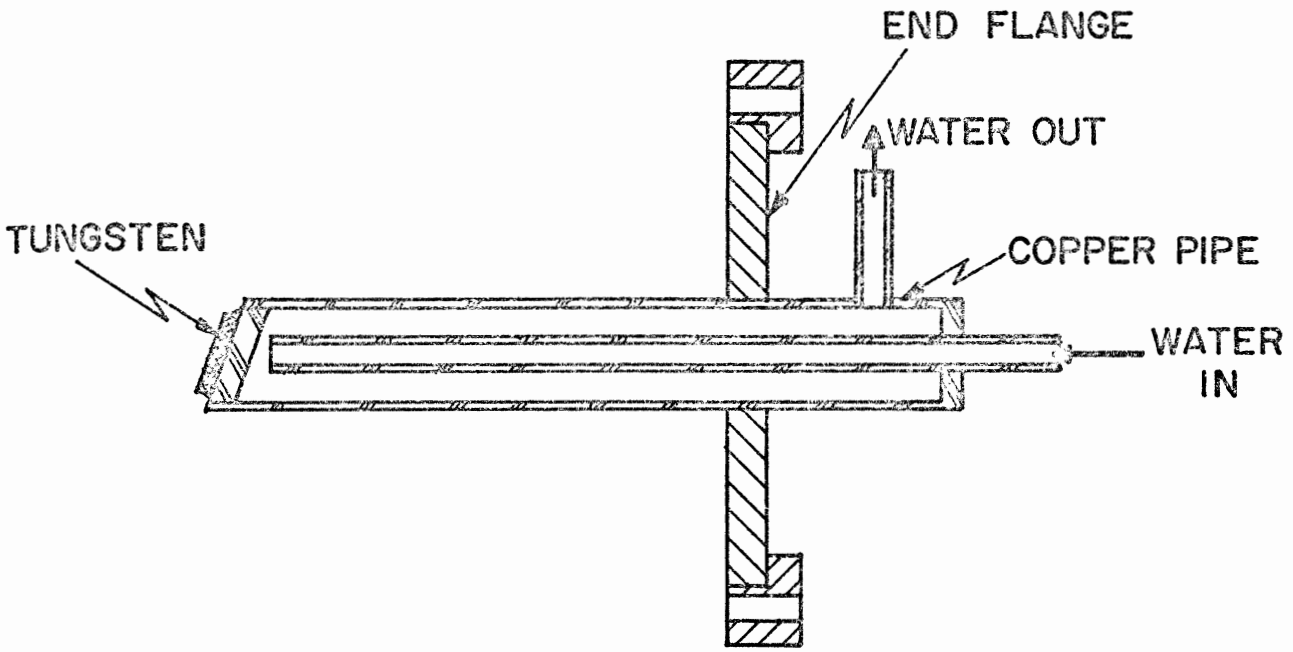
END FLANGE
WATER OUT
TUNGSTEN
COPPER PIPE
WATER
IN

(a)

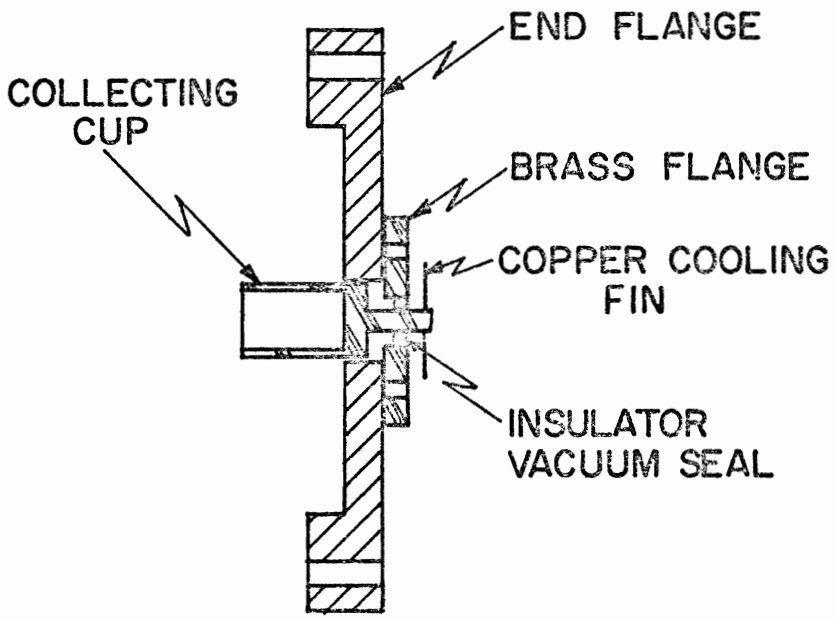
END FLANGE
COLLECTING
CUP
BRASS FLANGE
COPPER COOLING
FIN
INSULATOR
VACUUM SEAL

(b)

Figure 12

(a) and (b) Output of the ER as taken with interior Collecting Cup across 15 Ohms.
Vertical Sensitivity: 0.5 V/cm
Horizontal Scale: 0.02 μsec/cm

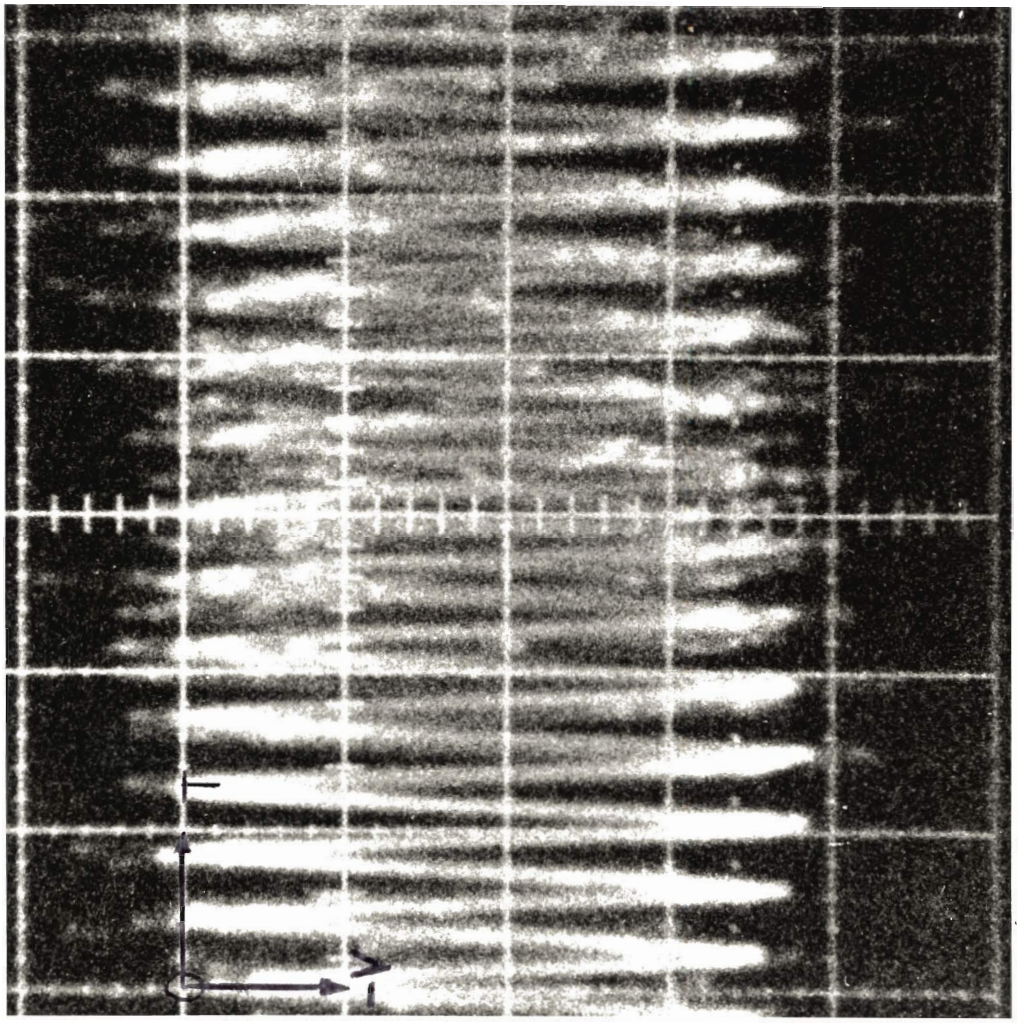
V
t

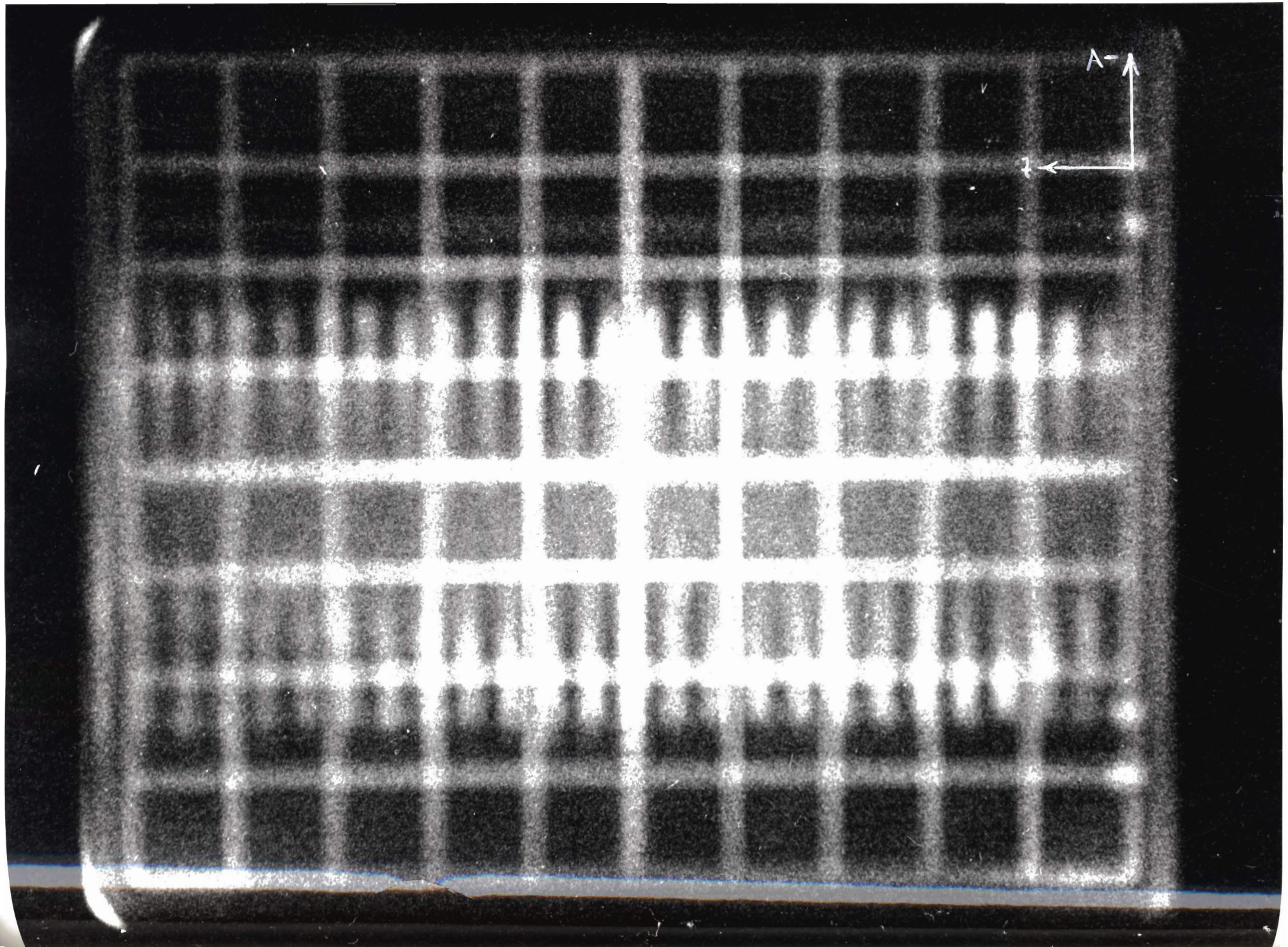
A
T

of 20 kV amplitude and 30 μsec duration. The vertical sensitivity was 0.5 V/cm and the time scale 0.02 μsec/cm (1 cm = 1 large division) corresponding to the maximum sweep speed of the scope. The time is increasing to the right and the pulse polarity is as indicated on the scope pictures. Unfortunately the speed of the time sweep was too fast for taking single sweep photographs. The exposure time actually was a multiple of the sweep period; the traces in the oscillograms therefore correspond to several successive pulse trains. The rise time of each pulse is about 5 nsec and slightly shorter than the decay time. The time elapse between two consecutive pulses hence is roughly 10^{-8} sec. Deflecting the beam by holding a bar magnet against the drift tube, turning off the focusing magnetic field, or the filament current invariably reduced the output to zero. Whenever measurements were taken, the operation of the ER was repeatedly checked in this way.

3-2. Measurements Outside the ER.

As already mentioned, only electrons of energies exceeding 524 keV can be expected to pass through the exit window. To measure the current formed by these electrons, a special tubular electrode was constructed (Fig. 9 (b)). Its design evolved from a series of trials. The cup that finally proved to be successful had a lead bottom to absorb high energy electrons, and was carefully shielded. It was mounted closely to the window, coaxially with respect to the axis of the ram, and its open side facing the window. Inserted between window and collector was a circular $\frac{1}{4}$ in.-thick lead baffle

with a concentric aperture of $\frac{3}{4}$ in. diameter to suppress photoelectric emission from the outer surface of the collector due to bremsstrahlung. The collector terminal was connected via a shielded cable to a Keithley electrometer, Model 610 A. To check what effect x-rays would have on the reading, the collector assembly was exposed to x-rays. The electrometer invariably showed a positive reading. That means that photoemission as well as secondary emission would reduce the electronic current rather than enhance it. The cathode was pulsed with a square wave of 20 kV-amplitude, 100 Hz-frequency, and a width of 30 μsec, as evident from the oscillogram in Fig. 13. The beam current was about 350 mA. As expected the average current indicated by the electrometer was negative and small, amounting under optimal operating conditions to only 10^{-10} A. This is not surprising in view of the fact that the acceleration process occurs, as further tests revealed, only during approximately 10 μsec of each pulse; that is within the time interval during which the cathode voltage happens to be at least -20 kV. In brief, the entire duration of the acceleration process is only 1 msec. In order to examine the output of the ER with the oscilloscope, the collector was connected to a Simtec charge sensitive pre-amplifier, Model P-11GP, which fed into the vertical input of a Tektronix oscilloscope, type 543 A. The ER was operated in the same manner as before. The single sweep oscillogram in Fig. 14 shows the output of the pre-amplifier which had unity gain and inverted the polarity of the input signal. The slow sweep (2 msec/cm) was

Figure 13

Voltage Pulse on the Cathode.

Vertical Sensitivity: 8000 V/cm

Horizontal Scale: 10 μsec/cm

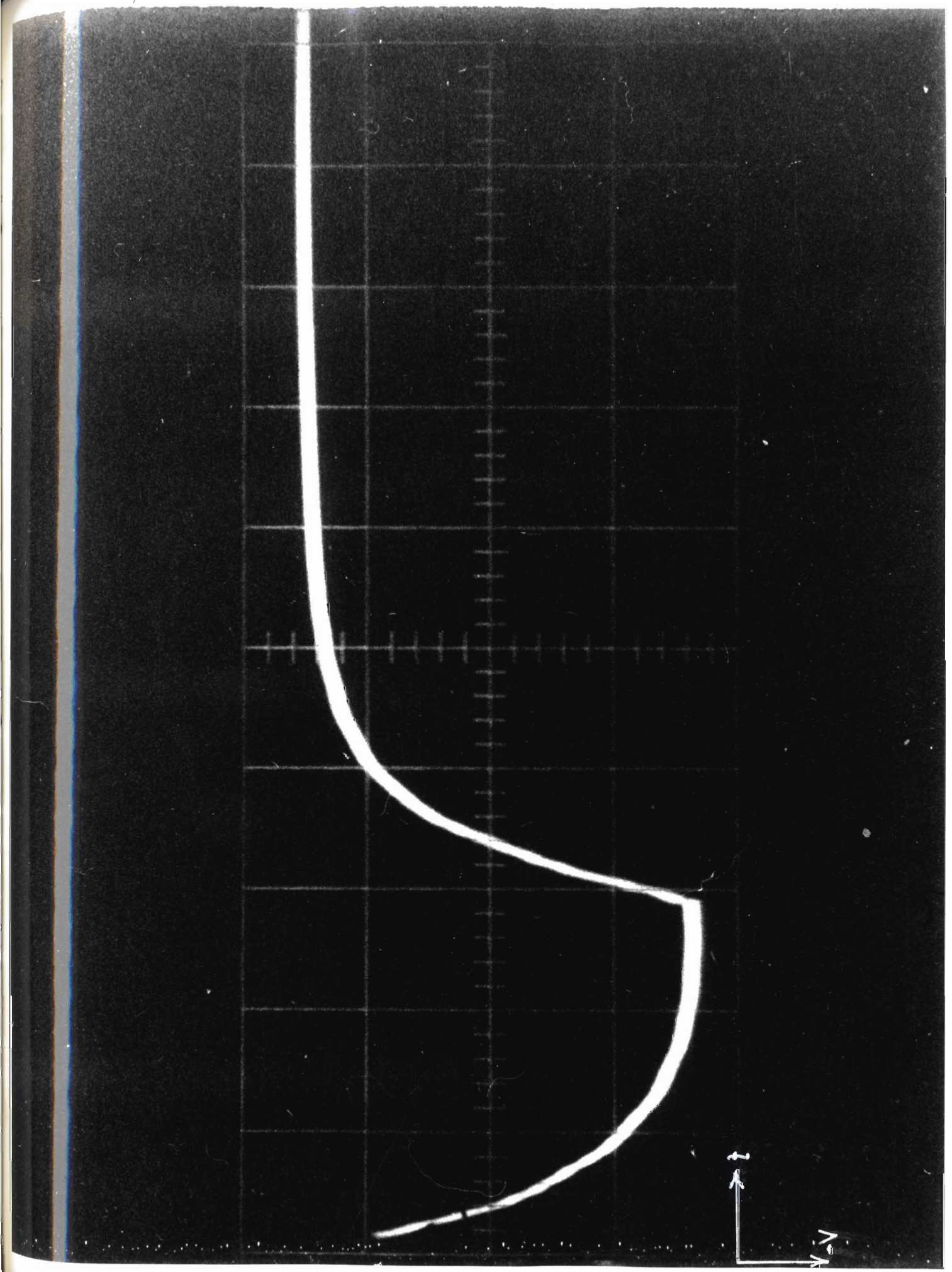

chosen to display the temporal separation between successive pulses which, of course, had to be the same as that of the voltage pulses applied to the cathode. The time is increasing to the right, negative voltages pointing upward, and the vertical sensitivity is 0.1 V/cm. To check on the influence of the pre-amplifier on the shape of the pulses, the collector output was fed directly into the oscilloscope. Comparing the results obtained with and without pre-amplifier, apart from the polarity inversion, no significant difference was found. The time constant RC of the external circuit was of the order of 10^{-4} sec. Hence $fRC >> 1$, where $f = 10^{8}$ Hz, i.e. the frequency of occurrence of the RE. The circuit therefore performed the operation of integration with respect to time of the current intercepted by the collector. Consequently the oscillogram shows qualitatively the electronic charge of the collector as a function of time. Of physical significance in this study is the charging up process which appears to be extremely short relative to the decay of the charge. Particularly interesting is the rate of increase of charge, since this is equal to the average collector current during the growth of charge. To get more information about rise time, average current and duration of current, another series of measurements was taken. The experimental set-up for these measurements was as follows: The lead collimators described in section 2-2 were put into position. In front of them, at an axial distance of about 5 cm, a simple electromagnet was placed in such a position that the collimated electron stream had to pass through

Figure 14

Output pulse of the ER taken with the Exterior Collecting Cup and Simtec Pre-amplifier P-11GP.

Vertical Sensitivity: 0.1 V/cm

Horizontal Scale: 2 msec/cm

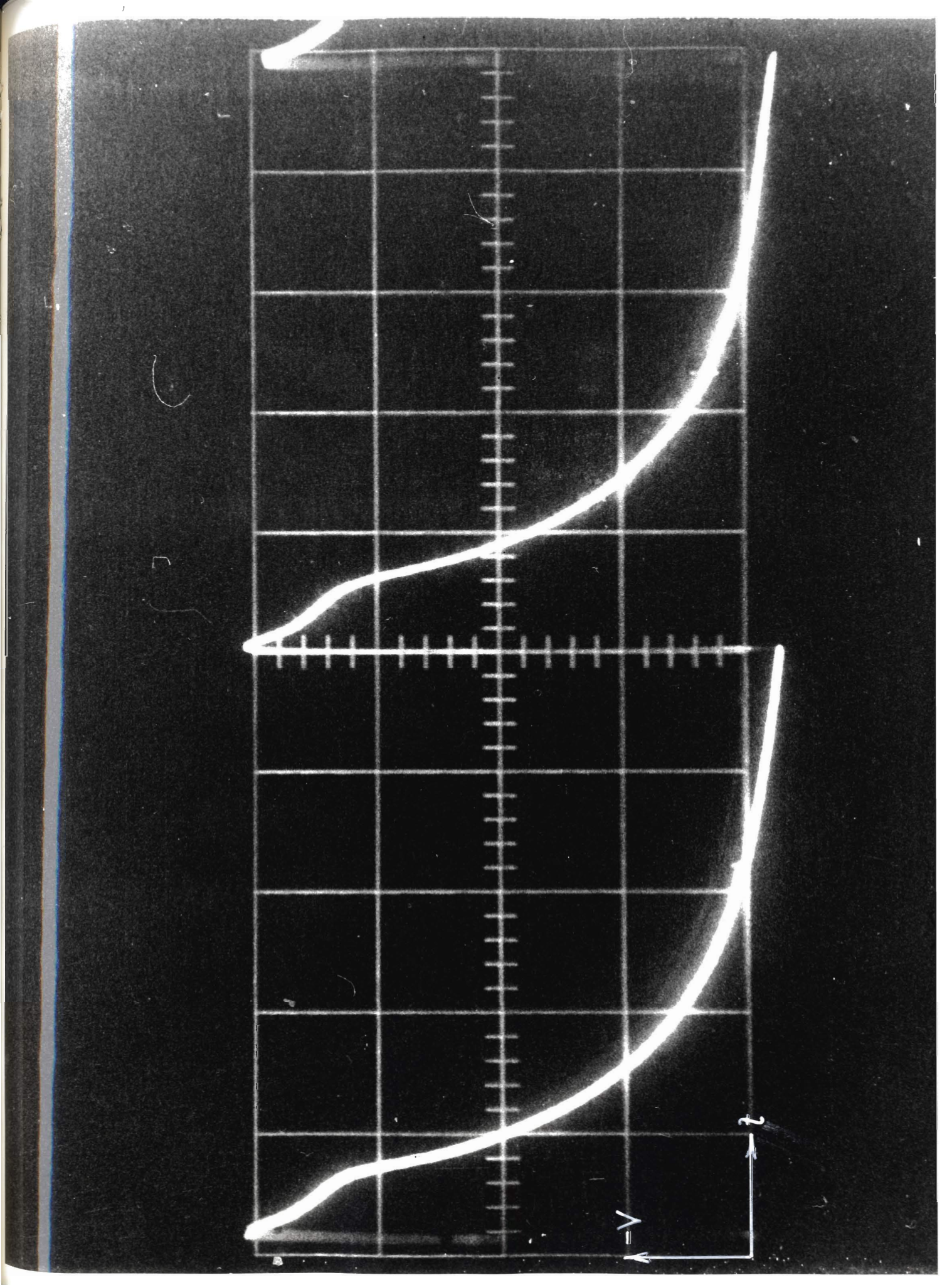
-V
I

the $\frac{1}{4}$ in. air gap between the circular pole pieces of 6.5 cm diameter. The graph in Fig. 15 presents the variation of the flux density B with radial distance r from the center of the air gap located at an axial distance of about 20 cm from the air gap in the direction of the beam and coaxially with respect to it was a Simtec Si(Li-drifted) detector, Model LC-50-2.0-30S, 2 mm thick, and an active area of 50 mm^2 perpendicular to the beam. This detector which was encapsulated to make it light tight, and biased with 500 V, was connected to the charge sensitive preamplifier of gain 1, which fed into the CRO.

Prior to the beam measurements, the detecting system was tested with the β-radiation of Cs^{137} and Co^{60}, and was found to function according to specifications. The scope traces corresponding to the detection of single electrons exhibited a rise time of about 50 nsec. This, however, is about 10 times longer than the rise time of the current pulses generated by the ER (Fig. 12). The active area of the Si(Li) detector was approximately the same as the cross-sectional area of the incident beam. The mean value of the beam current was found to be 10^{-10} A, hence the number of electrons impinging on the detector during operation was about 10^9/sec. In view of this fact, the detecting system could not be expected to resolve the output of the ER into distinct pulses produced by single electrons. In fact, it integrated the signals, as the scope photographs in Fig. 16 and 17 reveal. The picture in Fig. 16 was taken after insertion of an aluminum absorber (1564 mg/cm^2) between exit

Figure 15

Flux Density in Deflecting Magnet Gap

Current: 1 A.

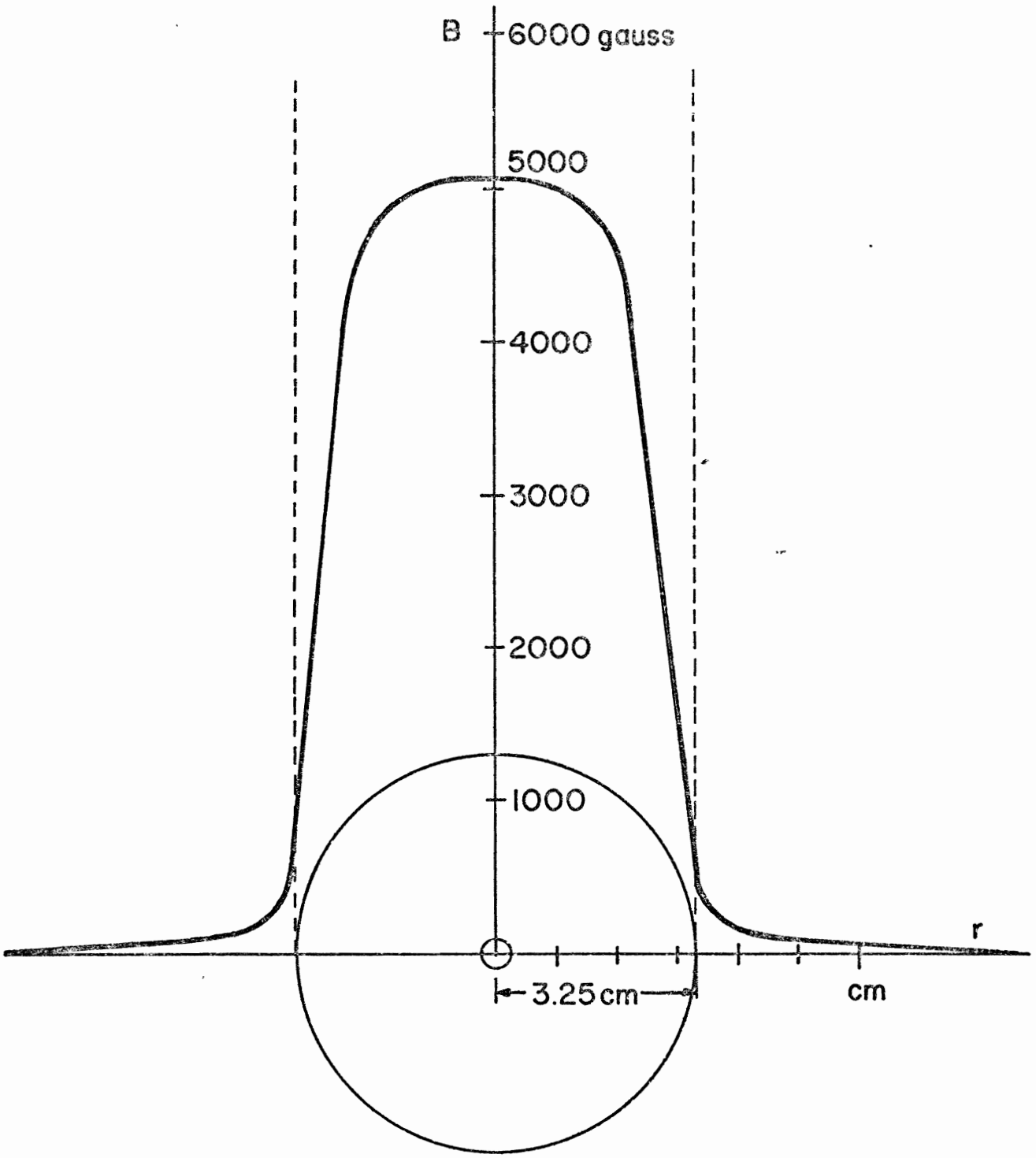
B
6000 gauss
5000
4000
3000
2000
1000
r
3.25 cm
cm

Figure 16

ER Output Pulse through Aluminum Absorber.

Scope triggered with Input Pulse to Cathode.

Pre-amp Output, Gain 4.

Vertical Sensitivity: 50 mV/cm

Horizontal Scale: 10 μsec/cm

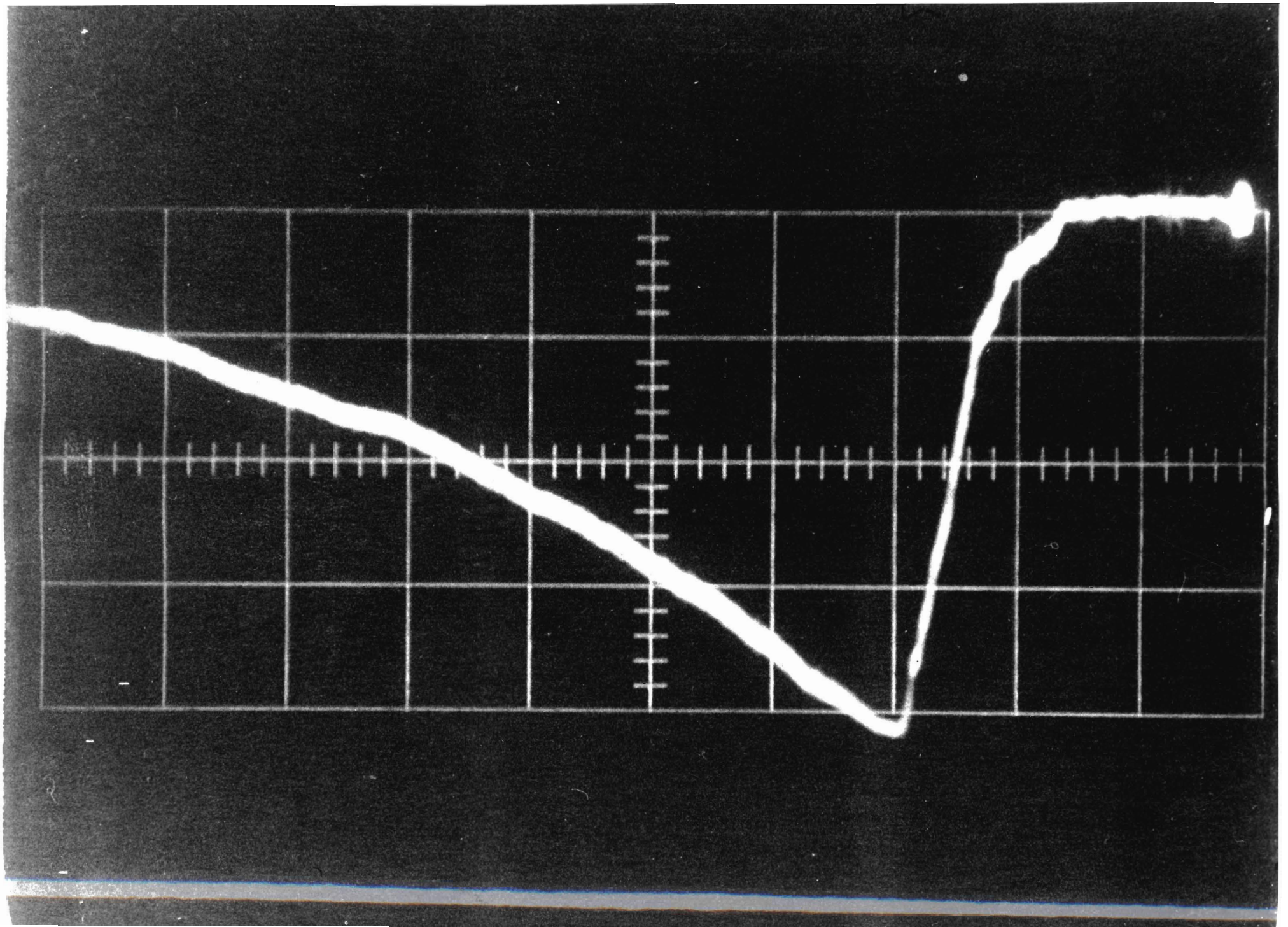

Figure 17

ER Output Pulse without Aluminum Absorber.

Scope triggered with Input Pulse to Cathode.

Pre-amp Output, Gain 1.

Vertical Sensitivity: 200 mV/cm.

Horizontal Scale: 10 μsec/cm

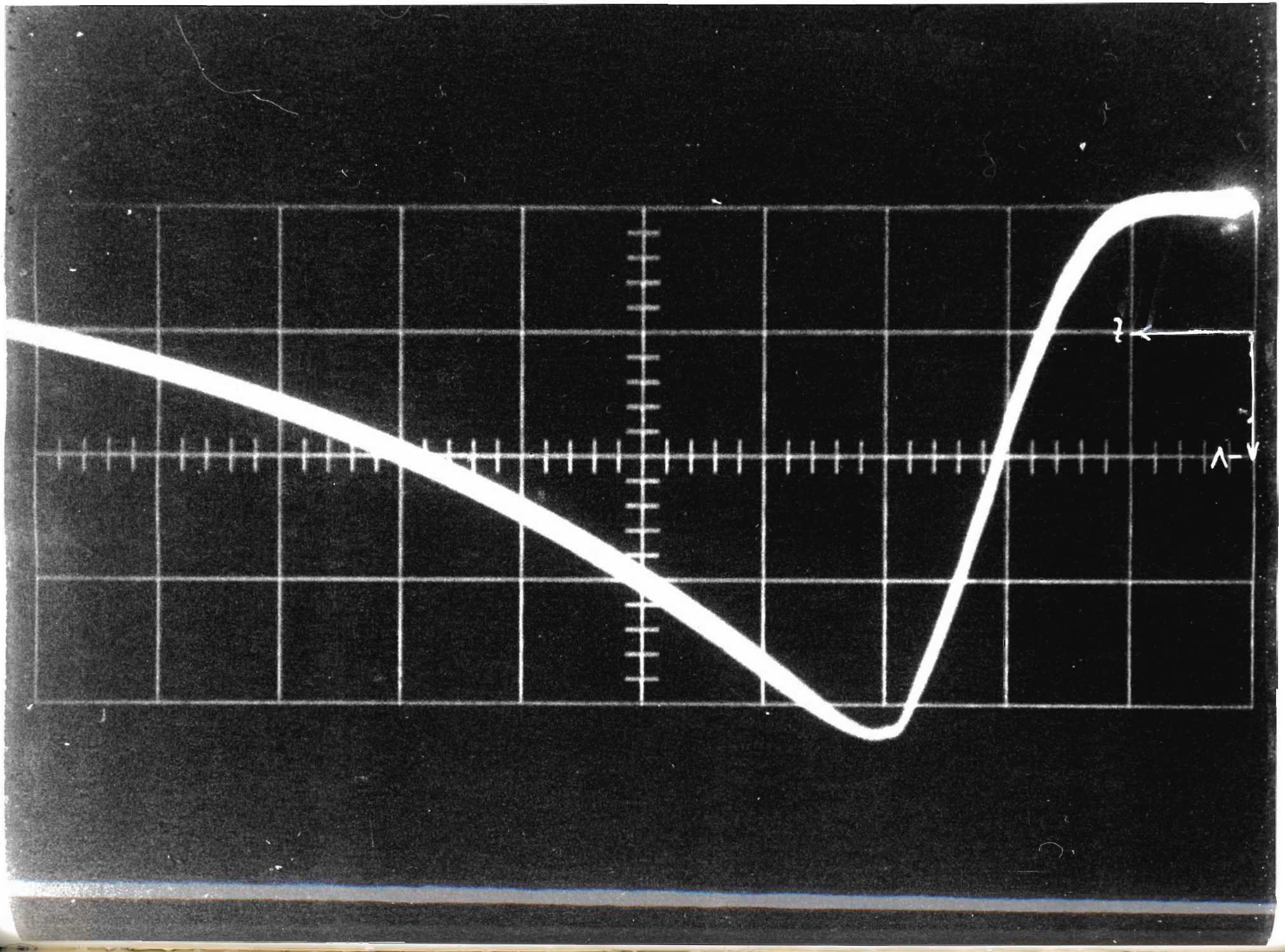

window and lead collimators. Taking the stopping power of the window and the air between window and detector into account electrons of energies above 3.8 MeV could reach the detector; the picture in Fig. 17 was obtained without absorber. The time scale is 10 μsec/cm, with time increasing to the right in both photographs, the vertical scale, however, is 50 mV/cm in Fig. 16, and 200 mV/cm in Fig. 17. The ER was operated in the same manner in both cases, but in the second case the detector was moved back, to prevent overloading of the pre-amplifier. The cathode voltage was applied 100 times per second for a period of 30 μsec; the voltage attained a maximum of -26 kV after about 20 μsec, and remained constant for the rest of the period. Looking at the oscillograms in Figures 16 and 17, one notices that the acceleration process occurs only after the cathode voltage has reached its peak value, that is during the last 10 μsec of each pulse width. The contribution of x-rays to the output of the detecting system was checked by energizing the electromagnet to deflect the electron beam as it passed through the air gap. It turned out to be negligibly small, as anticipated, since the Si(Li) detector was only 2 mm thick, and therefore relatively insensitive to x-rays.

As a matter of interest, the measurements were repeated after having modified the detecting system by inserting a linear amplifier and pulse shaper (Simtec Model M 31) between the pre-amplifier and oscilloscope. The linear amplifier was adjusted for the fastest possible pulse decay time, to remove the slow component in the

output of the pre-amplifier. The results of these measurements are presented in form of the oscillograms in Figures 18 and 19. They display a kind of "fine structure", which, however, seems to reflect the properties of the "electronics" rather than those of the input signal. A detailed interpretation of these scope traces was therefore not attempted.

Figure 18

ER Output Pulse through Aluminum Absorber.

Scope triggered with Input Pulse to Cathode.

Pre-amp plus Simtec M-31 Linear Amplifier.

Total Gain 8.

Vertical Sensitivity: 1 V/cm

Horizontal Scale: 10 μsec/cm

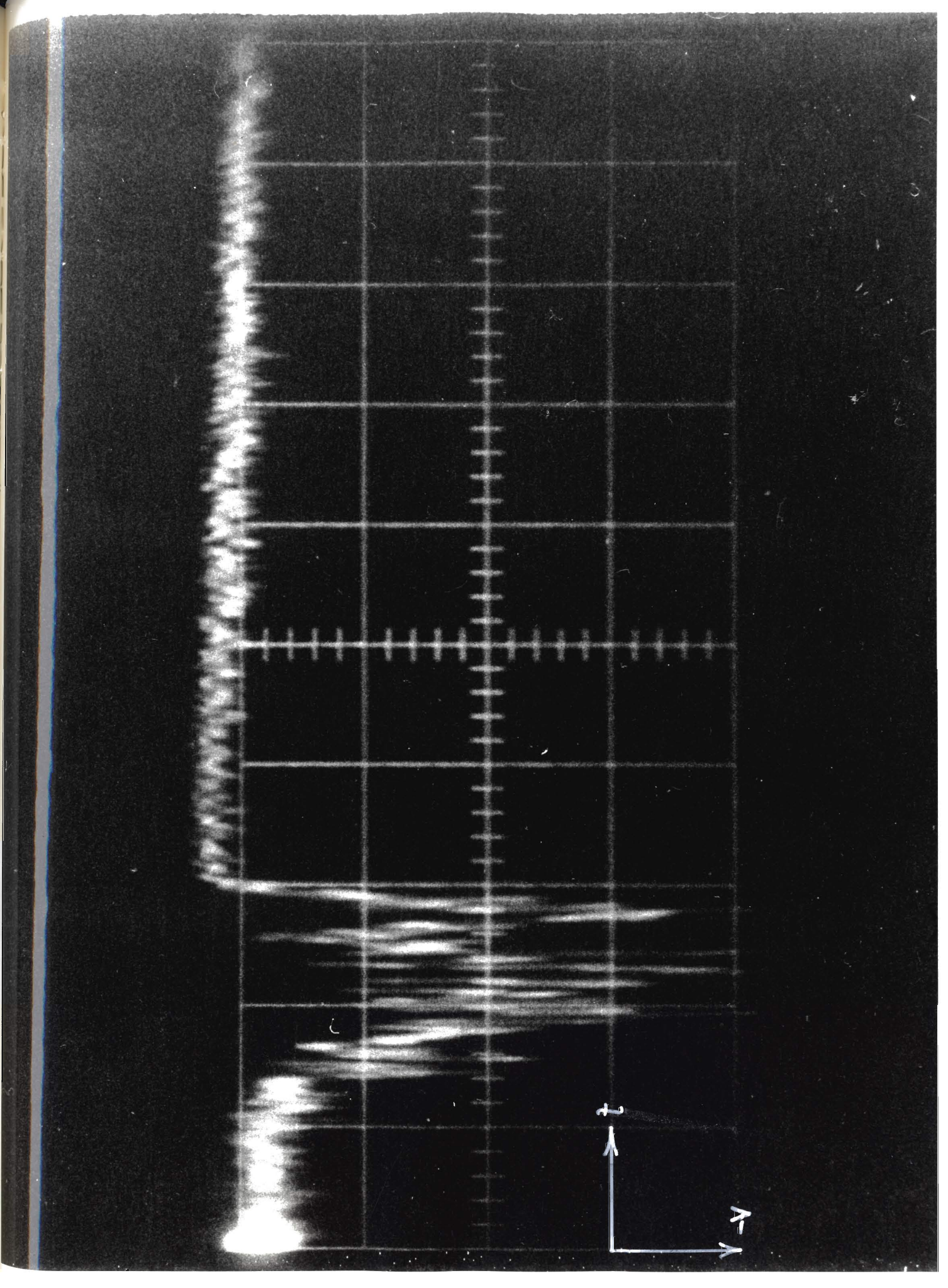

Figure 19

ER Output Pulse without Aluminum Absorber.

Scope triggered with Input Pulse to Cathode.

Pre-amp plus Simtec M-31 Linear Amplifier.

Total Gain 2.

Vertical Sensitivity: 2 V/cm

Horizontal Scale: 10 μsec/cm

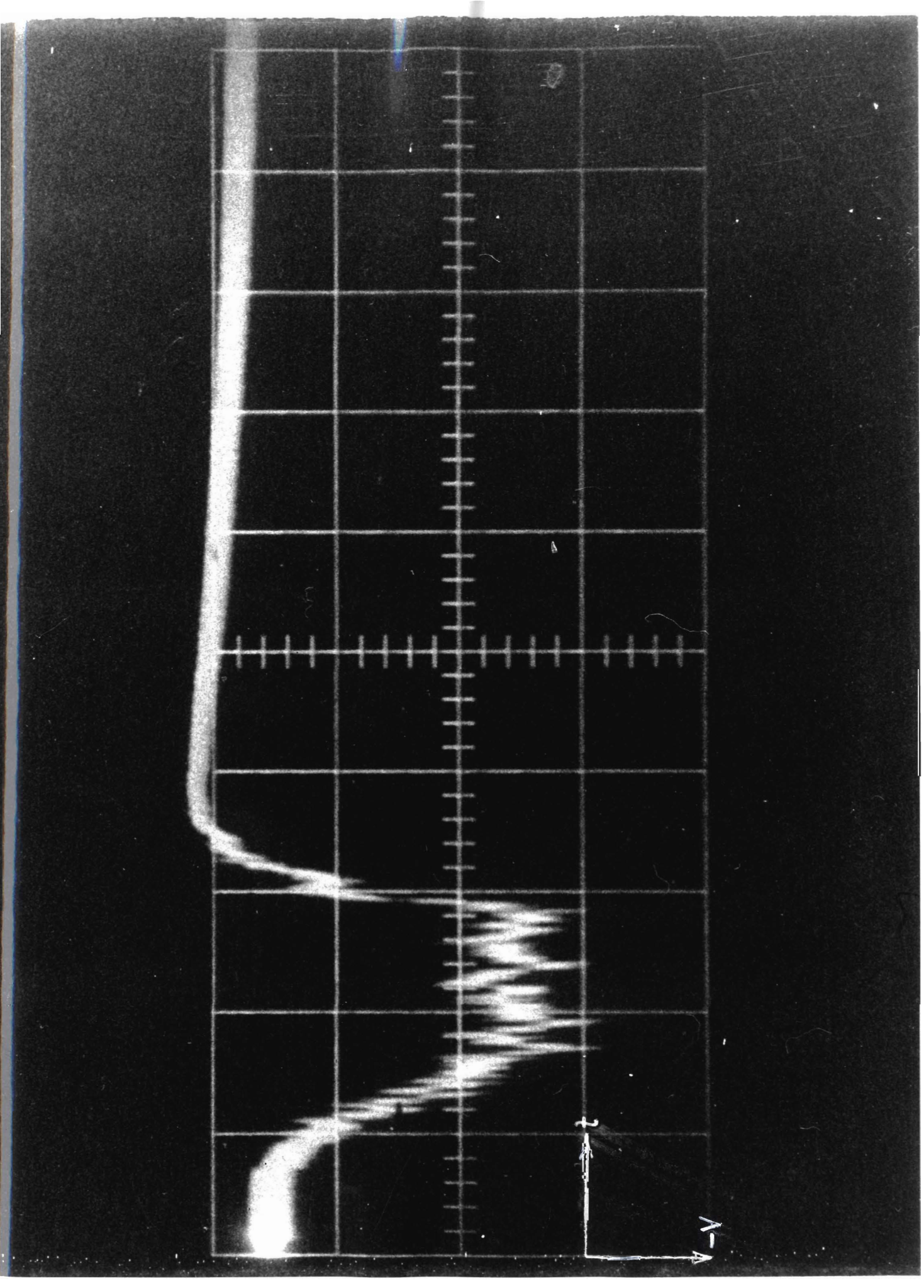

4. ENERGY MEASUREMENTS

4-1. Introduction.

In the ideal case all the energy invested in the electron beam would be transferred to the front electrons. The invested energy is given by $W_b = I\ U\ t$, I being the beam current, U the voltage applied to the cathode, and t the transit time, that is the time it takes the electrons in the beam to traverse the drift tube. The energy W_q of the accelerated electrons, constituting a charge q, may be expressed as $W_q = \frac{1}{2}\ q\ V = \frac{1}{2}\ C\ V^2$, where V denotes the energy level to which q is raised at the expense of the beam energy, and C a factor which for a given current density of the beam depends on the geometry of the system. Equating W_b and W_q gives $V = (2\ I\ U\ t/C)^{\frac{1}{2}}$. As the electrons that make up the charge q, gain momentum, the potential barrier which the virtual cathode represents, becomes smaller and smaller, receding along the beam into the drift tube until it vanishes. This recoiling of the potential barrier may be regarded as the reaction to the propulsion of the charge q. The energies of the electrons emitted into the decelerator will therefore range from V to zero electron volts. Taking into account the stopping power of the exit window of the ER, that of the detector window as well as that of the intervening air, only electrons of energies exceeding about 800 keV can be expected to be recorded.

4-2. Energy Tests.

For determining the energies of the electrons passing through the exit window, three fundamentally different methods were used.

The first method was based on magnetic deflection. The electron beam emerging from the exit window was collimated by three lead diaphragms and passed through the air gap of the analyzing electromagnet already described in the preceding chapter. The electromagnet served to produce in the air gap a homogeneous horizontal magnetic field (Fig. 15), transverse to the motion of the electrons. Its direction was such, that it deflected the passing electrons upward. At a distance of about 3 ft. from the air gap and about 1 ft. above the air gap in the vertical plane through the axis of the ER there was a NaI(Tl) scintillation detector. The electrons could enter the crystal only if their original direction of travel was rotated through a certain angle by the transverse magnetic field in the air gap. The set-up for the deflection measurement is shown in the photograph of the ER in Fig. 7. The knowledge of this angle and of the geometry allowed one to compute the energies of the electrons striking the detector.

The second method made use of the penetrating power of the electrons. The experimental arrangement was basically the same as for the deflection method, except that the detector was lowered and aligned with the axis of the system. Aside from this, the NaI(Tl) detector was replaced by the Si(Li) detector plus matching pre-amplifier. Aluminum disks, calibrated in mg/cm^2 were placed

between window and lead collimators. The minimum thickness of absorber which just prevented the electrons from passing to the detector was then determined. The transverse magnetic field was briefly applied during each measurement to check on the contribution of the x-rays to the background of the output. From the familiar relation between energy of the electrons and their range in aluminum, the energy of the fastest electrons in the signal could be readily computed.

The third method employed for determining the energies of the accelerated electrons is known as scintillation spectroscopy. Referring to the block diagram in Fig. 20, light from a scintillation produced by the passage of an electron in the thallium activated sodium iodide crystal releases photoelectrons from the cathode of the photomultiplier tube. This pulse of electrons is amplified by the dynode structure of the tube, so that an electrical output pulse is produced of sufficient magnitude to be amplified and operate various counting devices. The electrical output pulses are proportional or nearly proportional to the energy expended in the scintillator, that is to the energy of the impinging electron. Hence the pulse height increases with particle energy, so that with suitable calibration procedures the energy of a single charged particle may be determined from the size of the pulse. Naturally, other detecting systems can be used instead of that shown in Fig. 20.

This method appeared to be most convenient for studying

Figure 20

Block Diagram of Pulse Height Analysis System.

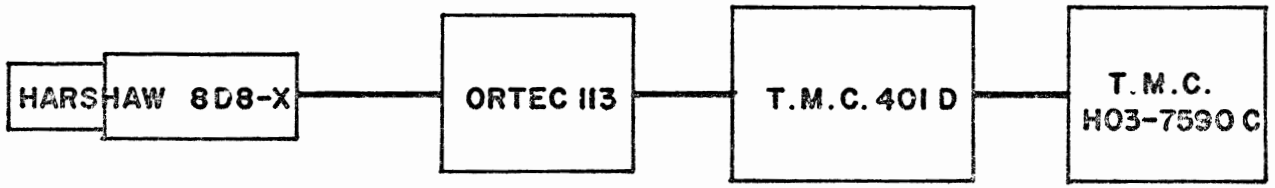

CRYSTAL + PHOTOMULTIPLIER PREAMP

PULSE
HEIGHT
ANALYZER

X-Y PLOTTER

both peak energies of the accelerated electrons and energy distributions under various operating conditions. However, in order to obtain satisfactory results, one has to see that the number of particles entering the detector does not exceed 10^4 per second, because of the limited time resolution of the detecting system. Preliminary measurements showed that if the active area of the detector is fully exposed to the output of the ER, the number of electrons hitting the detector is of the order of 10^9 per second. It was therefore decided to try to change the experimental arrangement in a way that only a small fraction of the output electrons could reach the detector. For example, the detector was placed about 10 ft. away from the exit window and slowly moved into the path of the beam, or the beam was passed through a hole in a block of lead, having a diameter of 2 mm and a length of 50 mm, and gradually deflected by a transverse magnetic field, scanning in this way the active area of the detector. None of these measures, however, proved to be fully successful. Scintillation spectroscopy was thus dropped after initial attempted use in this work as one of the methods of obtaining information about the energy and energy distribution of the electrons accelerated by the ER.

Originally it was planned to let the beam of high energy electrons impinge upon a tungsten target and determine their energies from measurement of the Bremsstrahlung. The construction details are shown in Fig. 11 (a). The flange holding the target was mounted in place of the exit window, which was placed on top of the auxiliary

port (Fig. 8). The tungsten target was thus positioned directly below the window and in the path of the beam. A scintillation detector placed above the window was thus able to "see" the x-rays produced by the electrons on the target. However these x-rays could not be resolved for reasons explained above, in addition it was found by deflection measurements that scattered high energy electrons were present in the output. These measurements also produced high radiation levels in the target area, and were thus discontinued.

The energy investigations involved also the study of the dependence of the energy range of the accelerated electrons on the various performance parameters, such as cathode voltage, beam current, flux densities of the applied magnetic fields, etc. As a result of this study, the optimal operating conditions, that is, the conditions under which for a given cathode voltage, the energy range of the output electrons attained a maximum, were established.

5. RESULTS AND DISCUSSION

All the energy measurements were carried out under the following operating conditions, which proved to be optimal:

Amplitude of the cathode voltage pulses	20 kV
Pulse repetition frequency	100 Hz
Duration of each pulse	30 μsec
Beam current	350 mA
Axial flux density at the cathode	15 G
Axial flux density along the drift tube	1000 G
Axial flux density at the decelerator	1500 G
Pressure	0.2 μTorr

5-1. Deflection Method.

An electron of charge e, moving with constant speed v through the air gap of the analyzing electromagnet, is deflected by a magnetic force $F = e\ v\ B$, where B denotes the flux density in the air gap. The angle α through which the path of the electron is turned varies with the mass m and speed v of the electron. If the angle α and the geometry of the experimental arrangement are known, the radius of curvature ρ of the electron path in the air can be computed. From the relation $\frac{mv^2}{\rho} = e\ v\ B$ follows for the momentum of the electron $p = e\ \rho\ B$. The energy E is given by the equation $E^2 = p^2c^2 + m_o^2c^4$, or in very good approximation for electrons in the MeV range by $E = pc = ce\rho B$. Hence the kinetic energy T, which is the quantity of interest, is given by $T = E - m_oc^2 = ce\rho B - m_oc^2$, c being the speed of light and m_o the rest mass of the electron. The angle α and the radius of

curvature ρ were the same for all deflection measurements and happened to be 20° and 17 cm, respectively. To determine the maximum energy of the electrons passing through the analyzing magnetic field, the flux density B was gradually increased until the signal dropped to the level of the background in the output of the detector.

A series of measurements was undertaken when the drift tube had a length of one meter. The flux density B required to deflect the most energetic electrons in the beam through an angle of 20° was on the average 1,650 G. Hence the average value of the quantity $B\rho$ turned out to be 2.8×10^{-2} Wb/m, and that of T = 7.9 MeV.

The corresponding results of the measurements when the length of the drift tube was 2 meters, were B = 2,600 G, $B\rho = 4.4 \times 10^{-2}$ Wb/m, and T = 12.7 MeV.

To these energy values one has to add 0.8 MeV, in order to account for the stopping power of the exit window, detector window and air between exit window and detector.

5-2 Absorption Method.

The total length of material an incident particle of given energy will travel before coming to rest, is called its range R. For the same velocity, the range is proportional to the mass of the incident particle, inversely proportional to the square of its charge, and inversely proportional to the electron density of the stopping material. Extensive tabulations of range curves

for different particles and absorbers are available. Also various empirical formulas have been devised; for example, for electrons, Feather's expression gives for the range of electrons in mg/cm^2 of aluminum $R = 543T - 160$; $0.8\ MeV < T < 3\ MeV$, where T is the initial kinetic energy of the electron in MeV.

The empirical formula used in this investigation was

$$R(mg/cm^2) = 530T\ (MeV) - 106$$

which covers the energy range $1\ MeV < T < 20\ MeV$.[6]

For the ER equipped with a drift tube of 1 m-length the range R in aluminum required to stop all the electrons emerging from the exit window turned out to be $4528.7\ mg/cm^2$. This corresponds to an energy of 8.75 MeV for the fastest electrons.

In the case of the ER with the 2 m-long drift tube the range R of aluminum needed to stop the incident electrons completely was found to be $6991.0\ mg/cm^2$, corresponding to an energy of 13.4 MeV for the fastest electrons.

5-3. Energy Distribution.

Initially the familiar method of pulse-height analysis was employed to investigate the energy spectrum of the accelerated electrons. When it was found, however, that the resolution time of the detecting circuit exceeded by far the temporal spacing between individual electrons, this convenient and elegant method had to be discarded. Instead, a simpler but much less instructive

and accurate procedure was used.

The experimental arrangement was the same as that for testing the maximum range of the accelerated electrons in aluminum. With the ER in operation, the range was gradually increased from zero to 5400 mg/cm^2 by inserting more and more absorbers between exit window and collimators until the scope traces could no longer be analyzed. The type of oscillograms obtained for the various ranges is shown in Figures 16 and 17. The increase of the voltage with time displayed on the scope screen is proportional to the growth of the incident charge. The slope of the voltage rise is therefore proportional to the rate of growth of charge, that is proportional to the incoming current. Hence relative changes of the slope will be equal to the corresponding relative changes of current. If, for example, lengthening of the path in aluminum causes a drop of the current by a factor 10, then the slope of the voltage rise will also decrease by a factor 10. From the scope pictures taken at different ranges, the corresponding slope values can be readily ascertained. With the aid of these data, the currents for various ranges can be calculated, if the current for one particular range is known. The range of the exit window is characterized by R = 350 mg/cm^2. For the sake of convenience it was decided to determine for this particular range the current which passed to the detector. As pointed out in chapter 3-2, the time average of the current passing through the exit window was found to be 10^{-10} A.

This results from current pulses which occur with a frequency of 10^8 Hz (Fig. 12) during time intervals of 10 μsec. Since the cathode was pulsed 100 times per second, there are 100 such intervals each second. If I_p denotes the amplitude of each pulse, then the mean value of the current during each of the 10 μsec intervals is about $\frac{1}{2}I_p$. The charge landing on the collector per second amounts to $\frac{1}{2}I_p \times 10^{-5} \times 100 = \frac{1}{2}I_p \times 10^{-3}$ C/sec. Equating this to the average current of 10^{-10} A, gives for the amplitude 2×10^{-7} A, and for the mean value of the current during the 10 μsec intervals 10^{-7} A. Using this value and the slope data obtained from the oscillograms, the currents corresponding to the various ranges in aluminum employed in this investigation could be calculated. The empirically found expression between range and energy allows one to relate these currents to the energies of the accelerated electrons. The graph in Fig. 21, in which the average current during the 10 μsec intervals is plotted vs. the energy, presents summarily the results of several series of measurements. Effects of scattering by the absorbers are not accounted for in this plot, but this does not mean that they are negligibly small. On the contrary, they may well be responsible for the relatively fast drop of current with increasing energy in the range up to 5 MeV. For example, the current formed by electrons of energies > 1 MeV is roughly 100 times larger than that composed of electrons of energies > 5 MeV, whereas the current due to electrons of energies > 6 MeV is only 10 times larger than that due to electrons of energies > 10 MeV.

Figure 21

Plot of Output Pulse Current versus Electron Energy

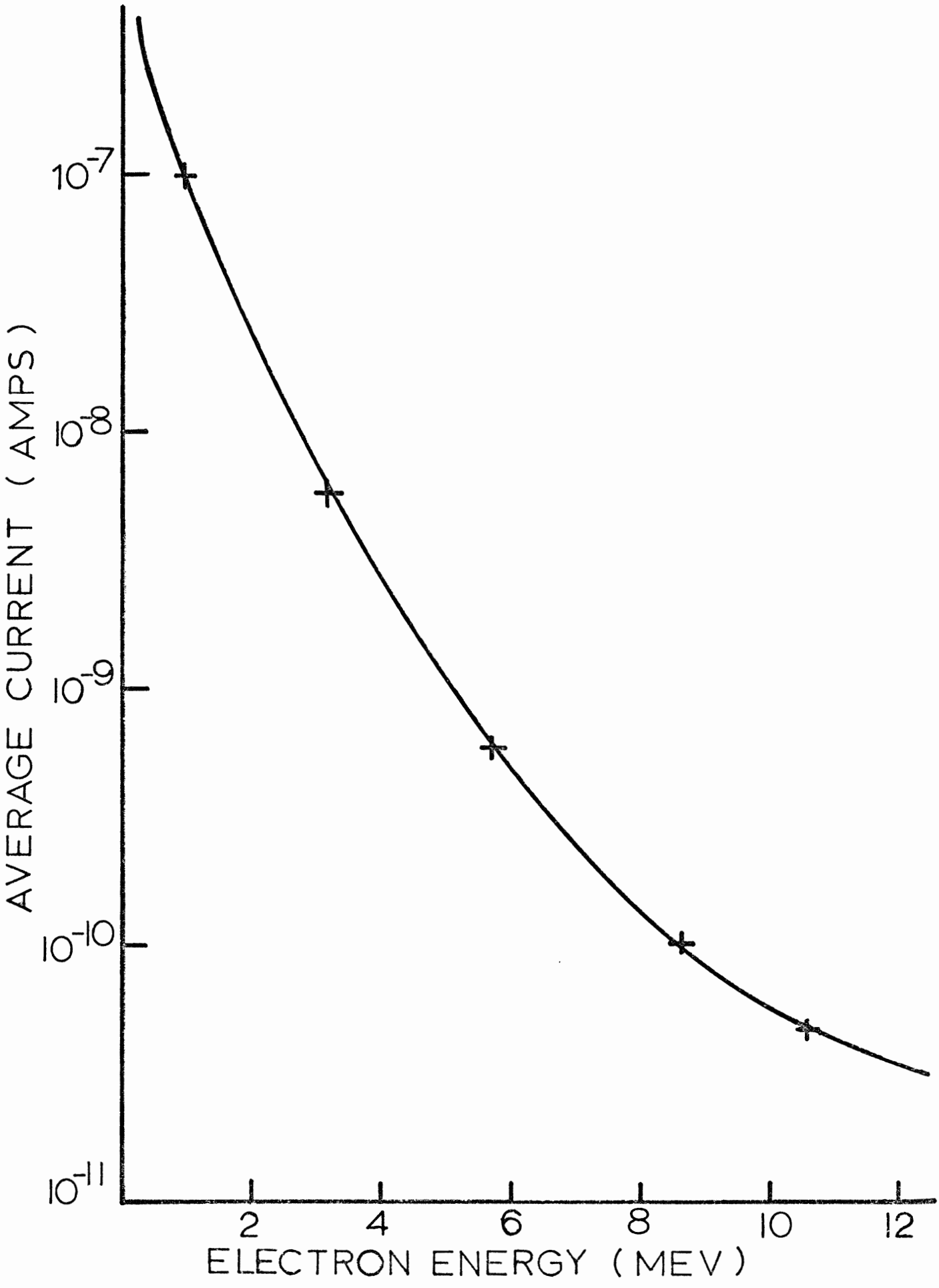
AVERAGE CURRENT (AMPS)
10-7
10-8
10-9
10-10
10-11
2
4
6
8
10
12
ELECTRON ENERGY (MEV)

5-4. Discussion.

All relevant results reported in the preceding sections were obtained by averaging over the results of several sets of measurements. The sets were repeated under identical operating conditions, but usually not on the same day. Often weeks or even months intervened between measurements of the same nature, nevertheless the deviations from the mean values presented in this work never exceeded ± 10%.

The energy level V to which the front electrons of the beam are lifted is given by $V = \eta(2\ I\ U\ t/C)^{\frac{1}{2}}$ (Section 4-1), where η is the coefficient of efficiency. Under the same operating conditions the transit time t is proportional to the length L of the drift tube. Therefore, if L is doubled, V should increase only by a factor $\sqrt{2}$. Actually it increased by a factor 1.5 as both deflection and absorption energy tests consistently showed. This discrepancy between theoretical and experimental value, surprisingly small, but persistent, confirms that the quantity C which has the dimension of a capacitance, depends on the geometry of the system. From the relation $V = \eta(2\ I\ U\ t/C)^{\frac{1}{2}}$, it follows that $C = 2\ \eta^2\ IUt/V^2$. Putting I = 350 mA, U = 20 kV, $t = 3 \times 10^{-8}$ sec, V = 10 MV and assuming $\eta = \frac{1}{2}$, one finds $C \sim 10^{-17}$ F. Hence the charge q of the capacitance, after being charged up to the voltage V is 10^{-10} A-sec. The distance between the end of the drift section and the exit window is about 0.3 m. The charge q will therefore reach the window within approximately 10^{-9} sec. This corresponds to a current of the order of 10^{-1} A, which is in good agreement with the exper-

imentally found value of 1.30×10^{-1} A (Fig. 12). Referring to Fig. 21, it is difficult to assess to what extent scattering by the absorber material is responsible for the relatively low external beam current. In any case, it will be desirable to raise this current as much as possible. One way to accomplish this would be to replace the presently used pure tungsten filament by an oxide coated cathode. It is known that under pulsed operation the thermionic emission of a conventional oxide coated cathode can attain current densities some factors of ten higher than under dc-operation.[7]

6. CONCLUSION

Summing up the measurements during testing showed that the ER performed according to the design. Since the design is based on the physical picture of the acceleration process, the successful operation of the ER proves the usefulness and validity of this picture. The present design of the machine served its purpose but should not be considered to be final. The installation of an indirectly heated strictly equipotential cathode would considerably improve the performance of the machine. The metal envelope of the device could be degassed and sealed prior to the mounting of the various solenoids. This would make pumping during operation superfluous and simplify the operation of the ER. Instead of lengthening the drift tube to accomplish acceleration of the electrons to higher energies, future development may lead to an arrangement of two or more ER's in series. The beam projected into and through the decelerator of the first ER would serve as the input beam of the next one in series. Apart from simplicity and efficiency, this novel acceleration method has the advantage of being applicable to all charged particles. The compactness, low cost and easy maintenance hold great promise for the ER to become a versatile and convenient radiation source with a wide field of application.

APPENDIX I

ELECTRON BEAM PARAMETERS

It is known that the motion of electrons in a combined electric and magnetic field can be determined by means of the standard Lagrange scheme, if $L(q_i,\dot{q}_i,t) = \frac{1}{2}mv^2 - eV + e(\vec{v}\cdot\vec{A})$ is used as the Lagrangian. The electron velocity $\vec{v}$, which for the beam electrons is small relative to c, the electric scalar potential V referred to ground, and the magnetic vector potential $\vec{A}$ become in this way functions of the general co-ordinates q_i, their time derivatives $\dot{q}_i$, and t. Since the system has axial symmetry, the cylindrical co-ordinates r, ϕ, and z are chosen. In the static case, where the potentials are independent of time, the Lagrangian equations may be written

$$\frac{d}{dt}\left(\frac{\partial L}{\partial \dot{q}_i}\right) = \frac{\partial L}{\partial q_i} \quad \text{or} \quad \dot{p}_i = \frac{\partial L}{\partial q_i} \tag{1}$$

where p_i designates the generalized momentum component, and

$$L(q_i, \dot{q}_i) = L(r, \phi, z, \dot{r}, \dot{\phi}, \dot{z}) =$$

$$= \tfrac{1}{2}m(\dot{r}^2 + r^2\dot{\phi}^2 + \dot{z}^2) - eV(r,z) + er\dot{\phi}A_\phi(r,z) \tag{2}$$

Hence the equations of motion

$$\ddot{r} = r\dot{\phi}^2 + kE_r + kA_\phi\dot{\phi} + kr\dot{\phi}\frac{\partial A_\phi}{\partial r} \tag{3}$$

$$\ddot{z} = kE_z + kr\dot{\phi}\frac{\partial A_\phi}{\partial z} \tag{4}$$

$$p_\phi = mr^2\dot{\Phi} + erA_\phi = \text{constant} \tag{5}$$

where $k = e/m$ and E_r and E_z are components of the electric field intensity $\vec{E}$.

$$\tfrac{1}{2}mv_o^2 = \tfrac{1}{2}m(\dot{r}^2 + r^2\dot{\Phi}^2 + \dot{z}^2) + eV \tag{6}$$

where $v_o = 2kV_o$, V_o being the potential of the cathode, and the relation

$$\vec{B} = \nabla \times \vec{A} \tag{7}$$

completely determine the properties of a cylindrical beam in an axial magnetic field.

It is not difficult to find the conditions under which a steady cylindrical beam of radius b can be produced and maintained in the drift tube, if V_o, B and the geometry of the system are given. From Eq. (7) it follows that

$$A_\phi = \tfrac{1}{2}rB \tag{8}$$

since $A_r = A_z = 0$. Since the length of the drift tube is very great in comparison to its radius R, the field intensity E due to the space charge can be considered as a function of r only. Equations (4) and (8) therefore give $\ddot{z} = 0$ and $\dot{z} = \text{constant}$. Provided the cathode is screened from the magnetic field, and

that the thermal velocities of the electrons can be ignored, the momentum p_ϕ at $z = 0$ is zero. As the momentum must be preserved, p_ϕ must be zero for $z > 0$ as well. The constant on the right-hand side of Eq. (5) is therefore zero. Consequently

$$\dot{\Phi} = \frac{-kA_\phi}{r} = -\tfrac{1}{2}kB \tag{9}$$

which shows that all electrons in the drift tube turn around the z-axis with the same angular velocity $\dot{\Phi}$. From Equations (8) and (3) it follows that $\ddot{r} = r\dot{\Phi}^2 + kE_r + krB\dot{\Phi}$.

The maintenance of a steady beam requires that both $\ddot{r}$ and $\dot{r}$ are zero. Hence

$$mr\dot{\Phi}^2 + eE_r + erB\dot{\Phi} = 0 \tag{10}$$

That means that the radial electric force eE_r, the Lorentz force $erB\dot{\Phi}$ and the centrifugal $mr\dot{\Phi}^2$ must compensate each other in order to give no radial acceleration and to maintain $\ddot{r} \equiv 0$. By inserting Equation (9) in (10), one obtains

$$E_r = \tfrac{1}{4}krB^2 \tag{11}$$

E_r on the other hand is related to the space-charge density ρ by Poisson's equation $\frac{1}{r}\frac{\partial(rE_r)}{\partial r} = \rho/\varepsilon_o$, which integrated gives

within the beam

$$E_r = r\rho/2\varepsilon_o \tag{12}$$

and with Eq. (11)

$$\rho = \tfrac{1}{2}\varepsilon_o kB^2 \tag{13}$$

To determine the axial velocity $\dot{z}$, Equations (6) and (9) are used. Thus

$$z^2 = 2kV_o - (\tfrac{1}{2}rkB)^2 - 2kV \tag{14}$$

The second integration of Poisson's relation provides the potential equations

$$V = \frac{\rho}{2\varepsilon_o} b^2 \ln(R/b) + \frac{\rho}{4\varepsilon_o}(b^2 - r^2) \tag{15}$$

within the beam, and

$$V = \frac{\rho}{2\varepsilon_o} b^2 \ln(R/r) \tag{16}$$

between beam and tube. Substituting (15) in (14) and replacing ρ by (13), one gets

$$\dot{z}^2 = 2kV_o - (\tfrac{1}{2}kbB)^2(1 + 2 \ln R/b) \qquad (17)$$

The total beam current is given by $i = \pi b^2 \rho \dot{z}$, or with (13) and (17)

$$i = \tfrac{1}{2}\pi b^2 \varepsilon_o k\{B^2[2kV_o - (\tfrac{1}{2}kbB)^2(1 + 2 \ln R/b)]^{\frac{1}{2}}\} \qquad (18)$$

The Equations (11), (13), (17) and (18) govern the existence of a steady cylindrical beam of uniform space-charge density ρ, in which the axial velocity of all electrons has the same value $\dot{z}$, and in which the space-charge repulsive forces are just balanced by the magnetic focusing forces, so that the beam may be made as long as desirable without any change in its cross-section. Equation (17), together with (9) indicates that the energy of the beam is partially transformed into rotational energy. The axial velocity diminishes with increasing B, and vanishes for $B = B_l$, where B_l designates the limit field which is defined by

$$B_l = \left[\frac{8V_o}{kb\ (1 + 2 \ln R/b)}\right]^{\frac{1}{2}} \qquad (19)$$

or

$$B_l = \frac{6.65\sqrt{V_o}}{b(1 + 2 \ln R/b)^{\frac{1}{2}}} \ G$$

with b in cm. and V_o in volts. No current can pass the tube, if $B \geq B_l$.

APPENDIX II

OPERATING INSTRUCTIONS

A II-1. Pump down from atmospheric pressure:*

(a) Turn on the forepump and thermocouple gauge.

(b) Open roughing valve to let forepump evacuate accelerator.

(c) When pressure reaches 100 microns, open foreline valve to diffusion pump and main valve. The roughing valve being closed, turn on the diffusion pump heater. Turn the heater control to maximum power (fully clockwise) to ensure rapid heating of the pump. The control can vary the power input to the heater from one-half to full power, and is normally set at full power during pump-down or operation. Only on stand-by is the heater power reduced to prevent deterioration of the diffusion pump oil.

(d) After 20 minutes of diffusion pump operation, turn on the ionization gauge, as the vacuum will be good enough to ensure its safe operation.

A II-2. Degassing procedures:

The accelerator works best at the highest possible vacuum. With this system, pressures of 2×10^{-7} torr during operation are easily achieved.

* It is assumed that the system is cold and that the diffusion pump was not exposed to the atmosphere, i.e. it is under vacuum and all valves are closed.

The electron gun, beam tube, decelerator and target area are self-degassing during operation. They are heated both thermally and by electron bombardment. The rest of the system may be degassed by external heating with a heat gun producing fairly high degassing temperatures.

A II-3. Rapid cycling:

Isolate the system completely from the vacuum pumps by closing the main valve. Air, or preferably dry nitrogen, may then be admitted through the air valve.

To pump down again, close the air valve, and follow the steps of A II-1, but note that the diffusion pump is hot and commences pumping immediately upon opening of the main valve.

A II-4. The focusing coils:

The main focusing coils consist of four sections, the inner and outer coils of section 1, nearest the gun, and the inner and outer coils of section 2, nearest the decelerator. They are energized by the powersupplies labelled accordingly.

The inner coils produce a field of 975 G at a current of 10 A, and the outer coils give 1025 G at 40 A.

The gap coil smoothes the magnetic field at the junction of the two accelerator sections. When only the inner coils are activated at full power, a gap coil current of 2 A assures uniformity of field. When inner and outer coils are at full power, a gap coil current of 3 A makes the field reasonably

uniform.

A II-5. The bucking coil:

The bucking coil surrounds the electron gun and controls the magnetic field there. With both inner and outer focusing coils operating, the stray magnetic field at the cathode surface is 105 G. An opposing current of 1 A in the bucking coil is needed to neutralize this field. The coil develops 100 G/A, which is added to or subtracted from the main focusing field at the cathode, depending on the direction of the current in the coil.

A II-6. The bunching coil:

The bunching coil surrounds the decelerator, and generates 200 G/A. Together with the focusing coil field, it produces, at full power, a flux density of 2500 G in the region just before the decelerator.

A II-7. A typical operating procedure:

Evacuate and degass until the pressure in the system is about 1×10^{-7} torr.

(a) Turn on Tektronix pulse generator, Cober high power pulse generator and monitoring oscilloscope. Allow to warm up for 5 minutes with Cober generator set at "HV READY".

(b) Turn on the filament and powersupplies of the solenoids. A panel light will indicate when filament preheating is completed.

(c) Set pulse generator to desired pulse length and

repetition rate (usually 30 μsec and 100 Hz, respectively). Do not exceed the 0.015 duty cycle of the Cober pulse generator.

(d) Energize the solenoids by turning on their powersupplies (see sections A II-4 to 6). Do not exceed the temperature ratings of the coils by prolonged operation. The bunching coil heats up faster than the other coils; the safe upper temperature limit of all coils is 160°C.

(e) Adjust the filament power to the appropriate value. The pointer of the dial before "top-center" assures space-charge limited operation; further increase in filament current will not increase the beam current, but reduce the life of the filament. IT IS IMPERATIVE THAT THE FILAMENT CURRENT IS ON BEFORE THE HIGH VOLTAGE (H.T.) IS APPLIED TO THE ELECTRON GUN, OTHERWISE THE H.T. TRANSFORMER IS NOT LOADED AND ITS INSULATION MAY BREAK DOWN.

(f) Slowly turn the high power pulse generator on and check pulse shape and voltage with the oscilloscope.

(g) The accelerator is now in operation. Check the vacuum during operation.

(h) To turn off, follow sequence of steps in reversed order, i.e. turn off H.T. etc.

NOTE: THE H.T. MUST BE TURNED DOWN BEFORE THE FILAMENT CURRENT, TO AVOID BREAK-DOWN OF THE H.T. TRANSFORMER.

A 11-8. Safety precautions:

As with any source of high energy particles, radiation safety precautions must be observed, and film badges worn during operation.

The danger zone of the ER extends from the exit window along the path the beam takes outside the ER. The radiation dose delivered facing the exit window is about 160 mR/sec or 576 R/h. Note that a dose of 400 R over the entire body is fatal.

Dangerous is also the high voltage supply for the electron gun, producing a peak voltage of 26,000 V at a current of 1 A. Extreme care must therefore be taken when handling any of the electron gun powersupplies.

BIBLIOGRAPHY

(1) Raudorf W.R., Wireless Engr. 28, 215 (1951).

(2) Billington I.J. and Raudorf W.R., Wireless Engr. 31, 287 (1954).

(3) Heese N.R. and Raudorf W.R., Brit. J. Appl. Phys. D 2, 717 (1969).

(4) Coutu A., Heese N.R., Raudorf W.R., J. Appl. Phys. 42, 4504 (1971).

(5) Convert G., Ann. Radioelect. 4, 279 (1949).

(6) Harrison A.W., Atomic and Nuclear Physics (MacMillan Co. of Canada, Toronto, 1966) Chap. 7, p. 132.

(7) Coomes E.A., J. Appl. Phys. 17, 647 (1946).